J. Fluid Mech. (1964), *vol.* 20, *part* 1, *pp.* 1–33
Printed in Great Britain

On the swimming of a flexible plate of arbitrary finite thickness

By J. P. ULDRICK† AND J. SIEKMANN

Advanced Mechanics Research Section, College of Engineering,
University of Florida, Gainesville, Florida, U.S.A.

(Received 4 November 1963)

This paper studies the effect of profile thickness on the propulsive forces generated by the swimming of a two-dimensional fish. Comparison of numerical calculations with reported experimental data shows good agreement and demonstrates a decrease of thrust with increasing thickness. Previous two-dimensional linearized theories on fish propulsion dealing with the motion of an infinitesimally thin hydrofoil are included in the present contribution as special cases.

1. Introduction

The swimming of sea animals as simulated by an infinitely thin two-dimensional waving plate has been discussed recently by several authors. Of particular interest to this investigation are the works of Lighthill (1960*a*, *b*), Smith & Stone (1961), Wu (1961, 1962), Kelly (1961), Siekmann (1962, 1963), Bonthron & Fejer (1962) and Siekmann & Pao (1964).

The present paper treats the case in which the thickness of the two-dimensional fish is taken into consideration in calculating the forces generated by the swimming motion of the fish.

2. Statement of the problem

Consider a flexible solid plate of constant depth (chord), of infinite length (span), and of arbitrary finite thickness (profile) immersed in an inviscid incompressible fluid in an otherwise uniform flow of constant velocity U in the direction of the positive x-axis of a right-handed Cartesian co-ordinate system. The fluid occupies the entire infinitely extended space. The assumption of infinite span and finite chord implies that the flow field around the plate can be treated as two-dimensional. The plate or hydrofoil which simulates the motion of a fish is supposed to execute a perturbation motion of small amplitude in the transverse direction, i.e. the propulsion of the fish will be generated by small lateral displacements of its body. The configuration of the plate when there is no fluctuation is assumed to be symmetric with respect to the chord as shown in figure 1. Henceforth, this shape will be identified as the stretched-straight configuration or the base profile. The flow field around the stretched-straight configuration will be referred to as the base flow field. Shown in figure 2 is a position

† Present address: Department of Engineering Mechanics, Clemson College, Clemson, S.C., U.S.A.

of the hydrofoil at a certain instant during flapping. In order to approximate the shape of a fish with sufficient accuracy a model with a rounded nose and a sharp tail will be employed.

With the (x, y)-rectangular co-ordinate system fixed in the plate the mean camber line is given at any time t by

$$y_m = h(x,t) = \tfrac{1}{2}[y_u(x,t) + y_l(x,t)] \quad (x_L \leqslant x \leqslant x_T),$$

where y_u and y_l are the ordinates of the upper and lower surfaces of the plate respectively, and x_L and x_T are the leading and trailing edge projections on the x-axis, respectively. The function $h(x,t)$ will be referred to as the flapping function.

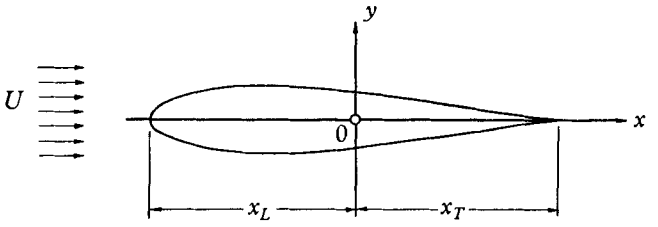

FIGURE 1. Stretched-straight configuration of the fish.

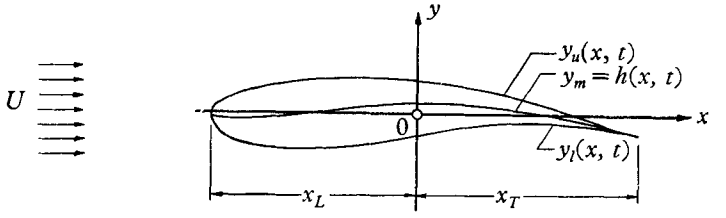

FIGURE 2. Displaced configuration of the fish.

Obviously, as a result of the displacement of the plate, the velocities of fluid particles on the upper and lower surface at the same x-co-ordinate will have different magnitudes. This velocity difference gives rise to a corresponding pressure difference and, as a consequence, there results a net unsteady hydrodynamic force which depends on the displacement and the rate of displacement of the plate. The component of this force along the x-axis will result in either a drag (directed in the positive x-axis) or a thrust (directed in the negative x-axis) for the fish.

The thrust is assumed to be generated by displacements forming a train of travelling waves of small amplitude which pass down the body of the fish from the head (leading edge) to the tail (trailing edge). The envelope of these waves varies arbitrarily along the length of the fish. We take the amplitude of these displacement waves to be a harmonic function of time. The magnitude of the thrust depends on the propagation velocity of these waves.

In the following the general theory for a flexible thick body undergoing preassigned undulations is developed on the basis of the complex velocity potential method. The body profile of the stretched-straight configuration in the physical plane is mapped by a suitable transformation into a circle and the unsteady

boundary conditions are satisfied by a source distribution on the circle. The problem is linearized by assuming a small unsteady perturbation theory. Due to the presence of the sharp trailing edge, the velocity induced at the tail by the source distribution possesses a singularity in the physical plane. This singularity is removed by introducing a fluctuating vortex distribution along the wake streamline of the steady base flow, such that the induced velocities of the source and vortex distributions combined vanish at the tail. With that, the so-called Kutta condition of a smooth attached flow with finite velocity at a sharp trailing edge is fulfilled. From the base flow potential, the source potential, and the vortex potential the pressure distribution on the base profile is determined by means of the Bernoulli equation for unsteady potential flow. With the pressure distribution known, the hydrodynamic forces acting on the hydrofoil can be calculated.

The thickness enters the problem through the mapping function in the form of a small thickness parameter. Finally, in computing the forces acting on the plate it was found to be convenient to linearize all functions with respect to the thickness parameter.

3. Mathematical formulation

The equations governing the two-dimensional motion of an inviscid and incompressible fluid are the continuity equation,

$$\operatorname{div} \mathbf{v} = \partial u/\partial x + \partial v/\partial y = 0, \tag{3.1}$$

and the Euler equation,

$$\rho\left(\frac{\partial \mathbf{v}}{\partial t} + \operatorname{grad}\frac{\mathbf{v}^2}{2} - \mathbf{v}\times\operatorname{curl}\mathbf{v}\right) = -\operatorname{grad} p. \tag{3.2}$$

In these equations we denote the velocity vector of a fluid particle near the profile by

$$\mathbf{v} = \{U + u(x,y,t),\ v(x,y,t)\},$$

where u and v are the perturbation velocities due to the deformation of the hydrofoil, ρ is the mass density and p the hydrodynamic pressure.

In the region of the flow field where the flow is irrotational we have the additional condition

$$\operatorname{curl}\mathbf{v} = \partial v/\partial x - \partial u/\partial y = 0. \tag{3.3}$$

This means that in this domain there exists a scalar point function $\Phi(x,y,t)$, called the (perturbation) velocity potential, which is defined by

$$u = \partial\Phi/\partial x, \quad v = \partial\Phi/\partial y. \tag{3.4}$$

Substituting equation (3.4) into the continuity equation leads to the Laplace equation for the velocity potential

$$\nabla^2\Phi \equiv \partial^2\Phi/\partial x^2 + \partial^2\Phi/\partial y^2 = 0.$$

Now the continuity equation can be integrated by introducing a stream function $\Psi(x,y,t)$, which is given by

$$u = \partial\Psi/\partial y = \partial\Phi/\partial x, \quad v = -\partial\Psi/\partial x = \partial\Phi/\partial y. \tag{3.5}$$

The equations in (3.5) are the familiar Cauchy–Riemann differential equations defining an analytic function, the complex velocity potential $F(z,t) = \Phi + i\Psi$ of the complex variable $z = x + iy$. From this function, the conjugate complex velocity $w(z,t) = u(x,y,t) + iv(x,y,t)$ can be found for any time t as

$$w(z,t) = \overline{\partial F/\partial z} = \overline{F'(z,t)}, \tag{3.6}$$

where the bar denotes the complex conjugate and the prime generally differentiation with respect to the independent complex variable. Hence, $F(z,t)$ completely determines the flow field.

Since it is a well-known fact in the theory of complex variables that an analytic function preserves its analyticity under a conformal transformation of coordinates, we determine the complex velocity potential of a flow field surrounding an infinite circular cylinder and transform this flow field into the flow field surrounding the 'fish'.

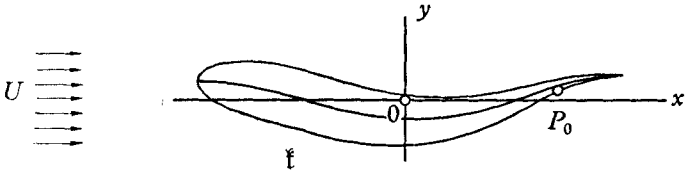

FIGURE 3. General profile configuration.

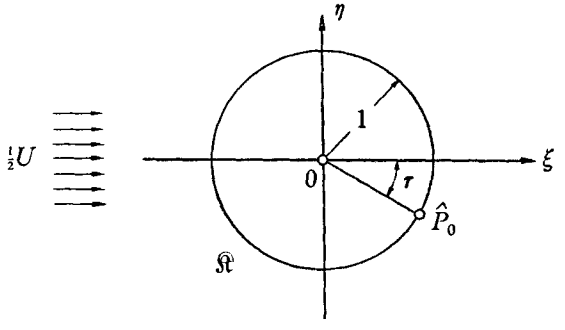

FIGURE 4. Circle plane for general profile configuration.

Let $z = f(\zeta)$ be a conformal mapping of the exterior of a unit circle $\mathfrak{K}$ in the $\zeta = \xi + i\eta$ plane to the exterior of the profile $\mathfrak{f}$ in the $z = x + iy$ plane, as shown in figures 3 and 4. The only limitation to be imposed on this function is that at a large distance from the origin the flow in the two planes differs at most by a constant, i.e.

$$\lim_{z\to\infty} w(z,t) = \tfrac{1}{2} \lim_{\zeta\to\infty} \hat{w}(\zeta,t).$$

Quantities in the ζ-plane are denoted by a circumflex. The factor $\frac{1}{2}$ in the foregoing equation is selected such that the chord of the base profile will be approximately two units.

As a model for the fish, it is reasonable to require that the profile has a rounded leading edge and a sharp trailing edge and that it be symmetric when in the stretched-straight configuration. For this basic configuration we wish to use a

symmetric Joukowski profile. This configuration can be mapped from a unit circle by the transformation

$$z = f(\zeta) = \frac{1}{2}\left[\zeta + \frac{(1-\epsilon)^2}{\zeta - \epsilon}\right] = \frac{1}{2}\left[\zeta + \sum_{n=1}^{\infty} \epsilon^{n-1}(1-\epsilon)^2 \zeta^{-n}\right], \tag{3.7}$$

where ϵ is a small non-negative quantity ($0 \leqslant \epsilon < 1$), respresenting a measure for the thickness of the fish. The thickness d of the fish at its mid-chord is approximately 2ϵ. Since the length l of the fish is approximately two, the thickness ratio

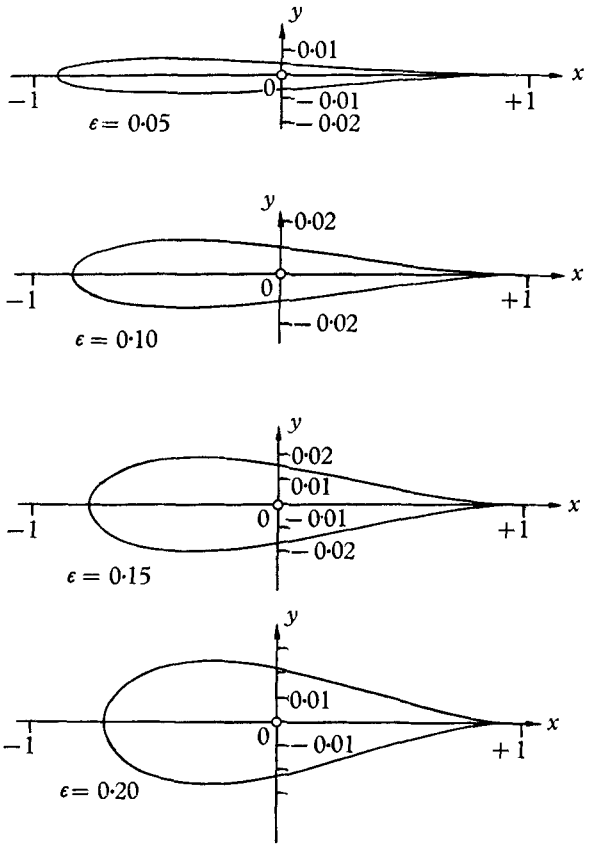

FIGURE 5. Stretched-straight configuration for several thickness parameters.

d/l at the mid-chord is of the order ϵ. In particular $\zeta = e^{i\vartheta}$ is the boundary of the circle and $z = f(e^{i\vartheta})$ is the boundary of the stretched-straight fish. Because of the fact that

$$df/d\zeta|_{\zeta=1} = f'(\zeta)|_{\zeta=1} = 0,$$

the function $f(\zeta)$ satisfies the physical requirement of a sharp trailing edge. Figure 5 shows the configuration of the base profile for several thickness parameters. The numerical values for the co-ordinates were calculated from equation (3.7) and are tabulated in table 1.

For the sake of application of the general theory later on we wish to investigate only profiles of small finite thickness and, as such, we shall assume that only the

linear effect in the thickness parameter ϵ is important. Hence, for this case, our mapping function $z = f(\zeta)$ can be written as

$$z = \frac{1}{2}\left[\zeta + \frac{1}{\zeta} - \frac{2\epsilon}{\zeta} + \frac{\epsilon}{\zeta^2}\right]. \tag{3.8}$$

Since the complex velocity potential is invariant under the given transformation

$$F(z(\zeta), t) = \hat{F}(\zeta, t),$$

$\epsilon = 0{\cdot}05$		$\epsilon = 0{\cdot}10$		$\epsilon = 0{\cdot}15$		$\epsilon = 0{\cdot}20$	
x	y	x	y	x	y	x	y
0·975	±0·000	0·950	±0·000	0·925	±0·000	0·900	±0·000
0·928	±0·001	0·906	±0·001	0·883	±0·002	0·860	±0·003
0·794	±0·006	0·778	±0·011	0·763	±0·017	0·747	±0·022
0·583	±0·017	0·579	±0·033	0·575	±0·050	0·570	±0·067
0·319	±0·033	0·328	±0·066	0·338	±0·099	0·347	±0·131
0·025	±0·050	0·050	±0·100	0·075	±0·150	0·100	±0·200
−0·269	±0·062	−0·228	±0·124	−0·188	±0·187	−0·147	±0·249
−0·533	±0·064	−0·479	±0·128	−0·425	±0·192	−0·370	±0·257
−0·744	+0·053	−0·678	±0·106	−0·613	±0·159	−0·547	±0·213
−0·878	±0·030	−0·806	±0·060	−0·733	±0·090	−0·661	±0·121
−0·925	±0·000	−0·850	±0·000	−0·775	±0·000	−0·700	±0·000

TABLE 1. Co-ordinates of the base profile.

the relation between the complex velocities in the two planes is given by

$$w = u + iv = \overline{\frac{\partial \hat{F}}{\partial \zeta}} \overline{\frac{d\zeta}{dz}} = \frac{\hat{w}(\zeta, t)}{f'(\zeta)}.\dagger \tag{3.9}$$

We assume that the unsteady lateral displacements $D(z, t)$ of the points P on the profile are small both in amplitude and in time rate and, as such, only the linear effects of the unsteady motion are of importance in determining the flow pattern and the forces acting due to the undulation of the hydrofoil. Therefore, we decompose the complex velocity potential into three parts as follows:

$$F(z, t) = F_0(z) + F_1(z, t) + F_2(z, t), \tag{3.10}$$

where F_0 is the potential of the uniform flow around the stretched-straight plate, F_1 is the contribution due to the unsteady motion of the profile and F_2 is the potential associated with the trailing vortices in the wake flow.

4. Pressure distribution

In order to determine the thrust, lift, and moment acting on the profile, we calculate the unsteady pressure distribution on the surface of the symmetric 'fish'. This can be accomplished by employing the unsteady Bernoulli equation

$$\partial\Phi/\partial t + \tfrac{1}{2}q^2 + p/\rho = \varpi(t), \tag{4.1}$$

† In order to avoid a cumbersome notation, especially when dealing with the conjugate complex function of $\hat{F}(\zeta, t)$, the circumflex will be occasionally omitted. Thus we shall set for example $\overline{\hat{F}(\zeta, t)} = \overline{F(\zeta, t)}$ and similarly $\overline{\partial\hat{F}/\partial\zeta} \equiv \overline{\hat{F}'(\zeta, t)} = \overline{\partial F/\partial\zeta}$.

which follows from the Euler equation (3.2) if the flow field is irrotational. Here q^2 denotes the square of the velocity and $\varpi(t)$ an arbitrary function of time which can be determined by the flow conditions at infinity.

Calculating

$$q^2 = \left.\frac{\partial \overline{F}}{\partial z}\,\frac{\partial F}{\partial z}\right|_{z=f(e^{i\vartheta})},$$

we arrive at

$$q^2 = \frac{\overline{dF_0}}{dz}\,\frac{dF_0}{dz} + 2\,\mathrm{Re}_i\left[\frac{\overline{dF_0}}{dz}\,\frac{\partial F_1}{\partial z}\right] + 2\,\mathrm{Re}_i\left[\frac{\overline{dF_0}}{dz}\,\frac{\partial F_2}{\partial z}\right] + 2\mathrm{Re}_i\left[\frac{\overline{\partial F_1}}{\partial z}\,\frac{\partial F_2}{\partial z}\right] + \frac{\overline{\partial F_1}}{\partial z}\,\frac{\partial F_1}{\partial z} + \frac{\overline{\partial F_2}}{\partial z}\,\frac{\partial F_2}{\partial z}, \tag{4.2}$$

where Re_i indicates the 'real part' operator with respect to the space imaginary unit i. The velocity potential Φ on the base profile follows from

$$\Phi = \mathrm{Re}_i\,[F(z,t)]_{z=f(e^{i\vartheta})}. \tag{4.3}$$

According to small unsteady perturbation theory, the last three terms in equation (4.2) may be neglected, since they are of second order in the perturbation velocities. Combining now equations (4.2) and (4.3) with the Bernoulli equation (4.1) and eliminating terms independent of time, the unsteady pressure distribution at a point P on the base profile becomes

$$\frac{1}{\rho}p(z,t) = -\,\mathrm{Re}_i\left\{\left(\frac{\partial}{\partial t} + \frac{\overline{dF_0}}{dz}\,\frac{\partial}{\partial z}\right)[F_1(z,t) + F_2(z,t)]\right\}_{z=f(e^{i\vartheta})},$$

which yields finally, in terms of the argument ϑ:

$$\frac{1}{\rho}\Pi(\vartheta,t) = \frac{1}{\rho}p(z(\zeta),t)_{\zeta=e^{i\vartheta}} = -\,\mathrm{Re}_i\left\{\left(\frac{\partial}{\partial t} + \frac{\overline{dF_0}}{d\zeta}\left|\frac{\partial\zeta}{\partial z}\right|^2\frac{\partial}{\partial\zeta}\right)[\hat{F}_1(\zeta,t) + \hat{F}_2(\zeta,t)]\right\}_{\zeta=e^{i\vartheta}}. \tag{4.4}$$

5. The complex velocity potentials F_0 and F_1

Consider the configuration of the profile as shown in figure 3. Since the mapping function for the profile is assumed to be known, it is only necessary to calculate the general potential for a flow around a circle and to map this flow field onto the profile. This complex potential can be written as

$$\hat{F}_0(\zeta) = \tfrac{1}{2}U\left(\zeta + \frac{1}{\zeta}\right) + \frac{i\hat{\Gamma}_0}{2\pi}\log\zeta,$$

where $\hat{\Gamma}_0$ denotes a circulation term. Then the conjugate velocity in the ζ-plane is given by

$$\hat{w}_0(\zeta) = \frac{\overline{dF_0}}{d\zeta} = \tfrac{1}{2}U\left(1 - \frac{1}{\bar{\zeta}^2}\right) - \frac{i\hat{\Gamma}_0}{2\pi}\frac{1}{\bar{\zeta}},$$

so that on the circle the velocity becomes

$$\hat{w}_0(e^{i\vartheta}) = \tfrac{1}{2}U(1 - e^{+2i\vartheta}) - \frac{i\hat{\Gamma}_0}{2\pi}e^{i\vartheta}.$$

Any point P on the profile in the z-plane is mapped into the point $\hat{P}$ on the circle in the ζ-plane by the transformation

$$z = f(e^{i\vartheta}).$$

Now let us assume that the position of the downstream stagnation point $P_0 \in \mathfrak{k}$ (figure 3) will be transformed into $\hat{P}_0 \in \mathfrak{K}$ (figure 4) by means of

$$\zeta = e^{i\tau}.$$

Since the velocity vanishes at $\zeta = e^{i\tau}$, the circulation can be found to be

$$\hat{\Gamma}_0 = -2\pi U \sin\tau.$$

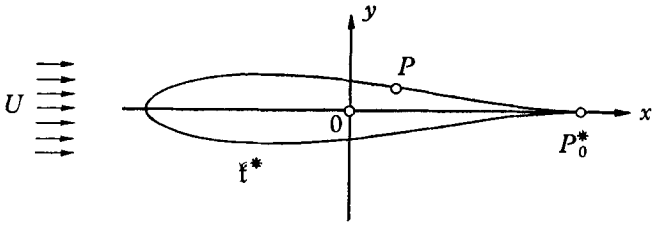

($z = x + iy$ plane)

FIGURE 6. Profile plane (z-plane).

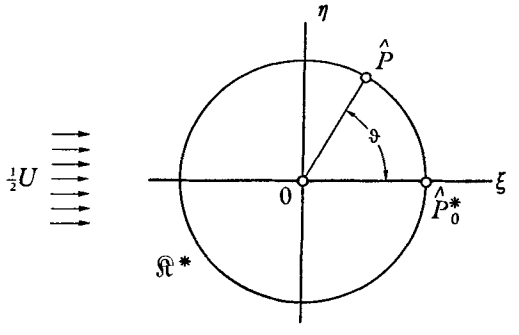

($\zeta = \xi + i\eta$ plane)

FIGURE 7. Circle plane (ζ-plane).

For a sharp trailing edge the Kutta condition requires that the flow leaves the profile smoothly; therefore, in order to satisfy this condition the downstream stagnation point must be located at the sharp tail. For the symmetric base profile $\mathfrak{k}^*$, as shown in figure 6, the sharp tail coincides with the x-axis and the downstream stagnation point $P_0^* \in \mathfrak{k}^*$ is mapped on the point $\hat{P}_0^* \in \mathfrak{K}^*$, which lies on the ξ-axis in the ζ-plane (figure 7). Thus, for this case, the circulation vanishes.

The complex velocity potential satisfying the steady-state boundary condition is

$$\hat{F}_0(\zeta) = \tfrac{1}{2}U(\zeta + \zeta^{-1}). \tag{5.1}$$

In order to determine the potential F_1 satisfying the unsteady boundary condition, we must first derive a relationship between the velocity of a point on the surface of the profile and the velocity of a fluid particle adjacent to this point. To

accomplish this, we let the unsteady displacement of a point P on the profile be denoted by $D(z,t)$. Then the position of this point at any time t is

$$z_P = z_{0P} + D(z,t), \tag{5.2}$$

where z_{0P} is the co-ordinate of the point on the stretched-straight configuration.

Now the boundary condition is given by the fact that the surface of the profile is a material impenetrable body, i.e. the velocity of a fluid particle in a direction normal to the boundary must be equal to the velocity of the corresponding point on the boundary in this direction. Therefore, we take the material derivative of equation (5.2) to obtain

$$\frac{dz_P}{dt} = \frac{\partial D}{\partial t} + \frac{\partial D}{\partial z}\frac{dz}{dt}, \tag{5.3}$$

where dz/dt is the velocity of the fluid particle at this point. Since the unsteady perturbation velocity is small, we make the hypothesis that the velocity of a fluid particle near the contour differs very little from the base flow velocity and thus can be approximated by the steady-state velocity at the boundary. This assumption seems reasonable at almost all points of the contour except in a small region around the stagnation points. Hence, the linearized unsteady boundary condition becomes

$$\frac{dz_P}{dt} = \frac{\partial D}{\partial t} + \overline{\frac{dF_0}{dz}}\frac{\partial D}{\partial z}. \tag{5.4}$$

Next, the complex unit tangent vector $\boldsymbol{t}$ to the boundary is given by

$$\boldsymbol{t} = \frac{dz}{|dz|} = \frac{1}{f'(e^{i\vartheta})}\frac{dz}{d\vartheta}, \tag{5.5}$$

and hence the complex unit normal vector $\boldsymbol{n}$ in an outward direction follows by a clockwise rotation about a right angle, yielding

$$\boldsymbol{n} = -i\boldsymbol{t}. \tag{5.6}$$

The velocity q_n of a point P on the surface of the profile in the normal direction is simply given by the scalar product of dz_P/dt and $\boldsymbol{n}$; thus we have

$$q_n(\vartheta,t) = \mathrm{Re}_i\left(-i\bar{\boldsymbol{t}}\frac{dz_P}{dt}\right). \tag{5.7}$$

Therefore, the corresponding velocity on the circle in the radial direction can be found to be

$$\hat{q}_r(\vartheta,t) = \mathrm{Re}_i\left(i\overline{\frac{dz}{d\vartheta}}\,\overline{\frac{dz_P}{dt}}\right),$$

or

$$\hat{q}_r(\vartheta,t) = -\mathrm{Im}_i\left(\overline{\frac{dz}{d\vartheta}}\,\overline{\frac{dz_P}{dt}}\right). \tag{5.8}$$

Im_i indicates the 'imaginary part' operator with respect to the space imaginary unit i. Now the undulatory motion of the profile is described by the flapping function $h(x,t)$. Here the x-co-ordinate refers to the base configuration. For a physical representation of fish swimming, this function is taken to be imaginary in the space variables, i.e. the lateral displacement is perpendicular to the real axis. Therefore, we arrive at the displacement function

$$D(z,t) = ih(x,t) \quad (x_L \leqslant x \leqslant x_T). \tag{5.9}$$

As pointed out earlier the propulsion is generated by a train of waves progressing astern with an amplitude depending on the spatial chord variable x. From photographs made of swimming salmonoid fish it seems to be reasonable to assume that generally the amplitude has its smallest value at the head and its largest value at the tail. We therefore postulate a displacement function of the form

$$D(z,t) = iH(x)\cos(\alpha x - \omega t + \Delta_0), \tag{5.10}$$

where α designates the wave number, ω the circle frequency (which is taken to be positive throughout this work), Δ_0 an arbitrary phase angle, and $H(x)$ the arbitrary amplitude of the envelope of the waves. It is convenient to subsume this motion under the most general form of the simple harmonic motion

$$D(z,t) = iH^*(x)\,e^{j\omega t}, \tag{5.11}$$

with $j = (-1)^{\frac{1}{2}}$ as the imaginary unit for the time variable t. It is not to be confused with the spatial imaginary unit i. Eventually, the real part in the time imaginary unit must be taken for physical interpretation.

Referring to equation (3.7) the x and y co-ordinates of point P on the base profile are given by

$$x = \frac{1}{2}\left[\cos\vartheta + \sum_{n=1}^{\infty} \epsilon^{n-1}(1-\epsilon)^2\cos n\vartheta\right],$$

and

$$y = \frac{1}{2}\left[\sin\vartheta - \sum_{n=1}^{\infty} \epsilon^{n-1}(1-\epsilon)^2\sin n\vartheta\right].$$

Since x is an even function of ϑ we can conclude that any function of x is even in ϑ, hence

$$h(x,t) = h[x(\vartheta),t] = h[x(-\vartheta),t] = h_1(\vartheta,t),$$

and also

$$H^*(x) = H^*[x(\vartheta)] = H^*[x(-\vartheta)] = H_1^*(\vartheta).$$

Therewith we can express the amplitude function $H_1^*(\vartheta)$ in a Fourier cosine series and write

$$H_1^*(\vartheta) = B_0 + 2\sum_{n=1}^{\infty} B_n\cos n\vartheta, \tag{5.12}$$

where

$$B_n = \frac{1}{\pi}\int_0^{\pi} H_1^*(\vartheta)\cos n\vartheta\,d\vartheta \quad (n \geqslant 0). \tag{5.13}$$

Now by substituting equation (5.11) into equation (5.4) we obtain first of all

$$\frac{dz_P}{dt} = i\left[j\omega H_1^*(\vartheta) + \frac{\overline{dF_0}}{dz}\frac{dH_1^*(\vartheta)}{dz}\right]_{z=f(e^{i\vartheta})} e^{j\omega t}.$$

Inserting this expression into equation (5.8) yields for the radial velocity $\hat{q}_r$ on the circle in the ζ-plane

$$\hat{q}_r(\vartheta,t) = -\operatorname{Im}_i\left\{\frac{dz}{d\vartheta}\,i\left[j\omega H_1^*(\vartheta) + \frac{\overline{dF_0}}{dz}\frac{dH_1^*(\vartheta)}{dz}\right]_{z=f(e^{i\vartheta})} e^{j\omega t}\right\}.$$

With

$$G(\vartheta) = \frac{1}{U}\left\{-\operatorname{Im}_i\left[\frac{dz}{d\vartheta}\,i\left(j\omega H_1^*(\vartheta) + \frac{\overline{dF_0}}{dz}\frac{dH_1^*(\vartheta)}{dz}\right)\right]\right\}_{z=f(e^{i\vartheta})},$$

the foregoing equation can be written in the compact form

$$\hat{q}_r(\vartheta,t) = UG(\vartheta)\,e^{j\omega t}. \tag{5.14}$$

With the help of equations (3.7) and (5.1), evaluated for $z = f(e^{i\vartheta})$, the function $G(\vartheta)$ can be put into the more convenient form

$$G(\vartheta) = -\mathrm{Im}_i\left\{e^{-i\vartheta}\left[\, jkf'(e^{-i\vartheta})\, H_1^*(\vartheta) - \frac{\sin\vartheta}{f'(e^{i\vartheta})}\,\frac{dH_1^*(\vartheta)}{d\vartheta}\right]\right\}, \tag{5.15}$$

where $k = \omega/U$ is the reduced frequency referred to the radius of the circle or, approximately, the half chord of the base profile. It can be shown that $G(\vartheta)$ is an odd function. Hence, we write it in the form

$$G(\vartheta) = 2\sum_{n=1}^{\infty} P_n \sin n\vartheta, \tag{5.16}$$

where the Fourier coefficients are given by

$$P_n = \frac{1}{\pi}\int_0^{\pi} G(\vartheta)\sin n\vartheta\, d\vartheta. \tag{5.17}$$

We satisfy the unsteady boundary condition for the radial velocity given by equation (5.14) by a source distribution along the circumference of the circle in

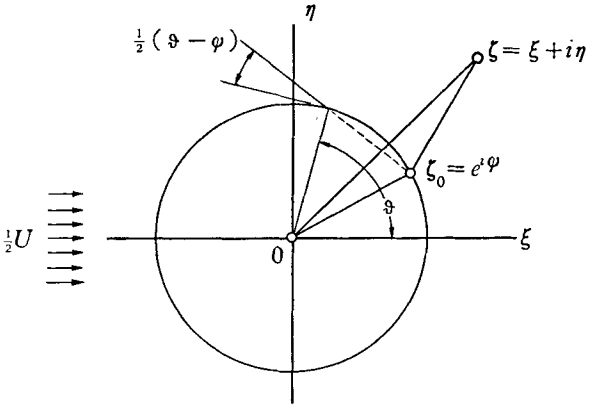

FIGURE 8. Circle plane with point source.

the ζ-plane or a corresponding source distribution along the surface of the symmetric profile.

Let the strength of this source distribution per unit arc length in the ζ-plane be denoted by $\hat{\mu}(\vartheta, t)$. This source distribution can be related, in an obvious way, to the radial velocity $\hat{q}_r(\vartheta, t)$ by

$$\hat{\mu}(\vartheta, t) = 2\hat{q}_r(\vartheta, t).$$

Then it is readily seen that the potential at a point ζ due to a point source of strength $\hat{\mu}$, located at ζ_0, is given by

$$(2\pi)^{-1}\hat{\mu}(\vartheta, t)\log(\zeta - \zeta_0).$$

Therefore, from figure 8, for the contribution to the total potential function $\hat{F}_1(\zeta, t)$ due to a point source at $\zeta_0 = e^{i\varphi}$, we arrive at

$$d\hat{F}_1(\zeta, t) = (2\pi)^{-1}\hat{\mu}(\varphi, t)\log(\zeta - e^{i\varphi})\, d\varphi,$$

and the total potential at ζ due to all sources becomes

$$\hat{F}_1(\zeta, t) = \frac{1}{2\pi}\int_0^{2\pi} 2\hat{q}_r(\varphi, t)\log(\zeta - e^{i\varphi})\, d\varphi,$$

or finally, by using equation (5.14):

$$\hat{F}_1(\zeta, t) = \frac{U}{2\pi} e^{j\omega t} \int_0^{2\pi} \dot{G}(\varphi) \log (\zeta - e^{i\varphi})^2 d\varphi. \tag{5.18}$$

6. The complex velocity potential F_2

For arbitrary undulations of the profile, the tangential velocity induced by the sources will not, in general, be finite at the sharp trailing edge and, as a consequence, the Kutta condition is violated. As an extension to the theory of Theodorsen (1934), we introduce a continuous vortex sheet located along the wake streamline of the steady-state flow with a distribution of image counter-vortices distributed in the interior region of the symmetric profile. These vortices and counter-vortices are introduced in such a way that Kelvin's theorem of total circulation is satisfied and that the net induced velocity on the boundary of the profile due to these vortices is tangent to the boundary. In addition, Helm-

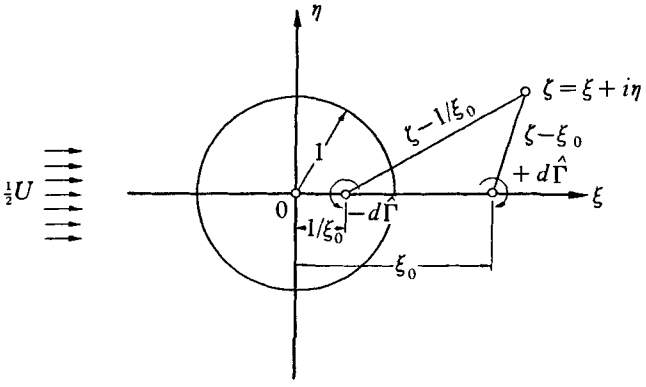

FIGURE 9. Circle plane with vortex pair.

holtz's law of persistence of vortex strength following a fluid particle is applied to a vortex element moving with a velocity approximately equal to the local steady-state velocity of a particle of fluid along the streamline emanating from the sharp tail. Finally, Kutta's condition is satisfied by requiring that the induced velocities due to the source potential and vortex potential combined vanish at the tail.

In order to develop the potential function which satisfies all the above requirements, we derive the potential function $\hat{F}_2(\zeta, t)$ arising from the associated vortex distribution in the circle plane. Shown in figure 9 is a single pair of vortices with equal strengths $d\hat{\Gamma}$—one located at $\zeta = \xi_0$ with a clockwise rotation which we take as positive, and the other located at the image point $\zeta = 1/\xi_0$ inside the circle with a counter-clockwise rotation. Clearly, the velocity induced by this vortex pair on the boundary of the circle is in a tangential direction and thus the corresponding induced velocity in the physical plane is tangent to the boundary of the symmetric hydrofoil. Furthermore, the total circulation is preserved by the introduction of this vortex pair since both are of equal strength but have

different directions of rotation. The potential $d\hat{F}_2$ at any point ζ due to this vortex pair is found to be

$$d\hat{F}_2 = \frac{i}{2\pi} d\hat{\Gamma} \log \frac{\zeta - \xi_0}{\zeta - \xi_0^{-1}}.$$

If we have a continuous vortex sheet of strength $\hat{\gamma}_w$ the circulation strength $d\hat{\Gamma}$ of the above pair of vortices can be related to the vortex strength distribution by

$$d\hat{\Gamma} = \hat{\gamma}_w d\xi_0.$$

Thus in the plane of the circle the complex velocity potential resulting from this vortex distribution is found to be

$$\hat{F}_2(\zeta, t) = \frac{i}{2\pi} \int_1^\infty \hat{\gamma}_w(\xi_0, t) \log \frac{\zeta - \xi_0}{\zeta - \xi_0^{-1}} d\xi_0, \tag{6.1}$$

where it is assumed that the unsteady motion has been going on for an infinite time.

We can relate this potential in terms of the corresponding vortex distribution in the plane of the profile by referring to the relation

$$\hat{\gamma}_w(\xi_0, t)\, d\xi_0 = \gamma_w(x_0, t)\, dx_0$$

between the circulation distribution in the ζ-plane to the circulation distribution in the z-plane. Then from the mapping function $z = f(\zeta)$ it follows that

$$dx_0 = (df(\xi_0)/d\xi_0)\, d\xi_0 = f'(\xi_0)\, d\xi_0,$$

and hence the desired relation

$$\hat{F}_2(\zeta, t) = \frac{i}{2\pi} \int_1^\infty \gamma_w(f(\xi_0), t) \log \frac{\zeta - \xi_0}{\zeta - \xi_0^{-1}} f'(\xi_0)\, d\xi_0. \tag{6.2}$$

We next apply Helmholtz's law of constancy of vortex strength following a fluid particle, namely

$$\gamma_w(x_0, t) = \text{const.}, \tag{6.3}$$

referred to a co-ordinate system moving with the particle of fluid. Therefore, the substantial derivative of γ_w is given by

$$\frac{d\gamma_w}{dt} = \frac{\partial \gamma_w}{\partial t} + \frac{\partial \gamma_w}{\partial x_0} \overline{\frac{dF_0}{dz}}\bigg|_{z=x_0} = 0. \tag{6.4}$$

However, since the unsteady perturbations are harmonic in time the vortex distribution can be written as

$$\gamma_w(x_0, t) = \gamma_w(x_0)\, e^{j\omega t}. \tag{6.5}$$

From the last two equations we obtain after some straightforward calculations

$$\hat{\gamma}_w(\xi_0) = \gamma_w(x_0 = f(\xi_0)) = \gamma_0 \exp(-jk\Theta), \tag{6.6}$$

where γ_0 is a constant, and Θ is defined by

$$\Theta = \Theta(\xi_0) = 2 \int_1^{\xi_0} \frac{[f'(\xi_0)]^2}{1 - \xi_0^{-2}} d\xi_0. \tag{6.7}$$

In order to derive the preceding formula, equation (5.1) was employed. Combining these results we get finally

$$\hat{F}_2(\zeta,t) = \frac{i}{2\pi}\gamma_0 e^{j\omega t}\int_1^{\infty} e^{-jk\Theta} f'(\xi_0)\log\frac{\zeta-\xi_0}{\zeta-\xi_0^{-1}}\,d\xi_0. \tag{6.8}$$

Now, in order to satisfy the Kutta condition we require that the tangential velocity on the circle vanishes at the downstream stagnation point which is located at $\zeta = 1$. This restriction implies that

$$\frac{\partial}{\partial\zeta}[\overline{F_1(\zeta,t)} + \overline{F_2(\zeta,t)}]_{\zeta=1} = 0. \tag{6.9}$$

Substituting the trigonometric series for $G(\varphi)$, given by equation (5.16), into equation

$$\left.\frac{\overline{\partial F_1}}{\partial\zeta}\right|_{\zeta=1} = \frac{U}{2\pi}e^{j\omega t}\int_0^{2\pi} G(\varphi)\frac{2}{1-e^{-i\varphi}}\,d\varphi$$

and separating the real and imaginary part in the space imaginary unit i we obtain, by employing the well-known integrals

$$\frac{1}{2\pi}\int_0^{2\pi}\sin n\varphi\,d\varphi = 0 \quad (n = 1,2,3,\ldots),$$

$$\frac{1}{2\pi}\int_0^{2\pi}\sin n\varphi\sin\varphi\,\frac{d\varphi}{1-\cos\varphi} = 1 \quad (n = 1,2,3,\ldots)$$

and after a few steps,

$$\left.\frac{\overline{\partial F_1}}{\partial\zeta}\right|_{\zeta=1} = -iU e^{j\omega t}\sum_{n=1}^{\infty} 2P_n. \tag{6.10}$$

Further it follows from equation (6.8) that

$$\left.\frac{\overline{\partial F_2}}{\partial\zeta}\right|_{\zeta=1} = -\frac{i}{2\pi}\gamma_0 e^{j\omega t}\int_1^{\infty} e^{-jk\Theta} f'(\xi_0)\frac{\xi_0-\xi_0^{-1}}{2-\xi_0-\xi_0^{-1}}\,d\xi_0. \tag{6.11}$$

Combining equations (6.10) and (6.11) with equation (6.9) we see that

$$iQ - i\gamma_0\,\mathrm{P}(jk;\epsilon) = 0, \tag{6.12}$$

where

$$Q = -U e^{j\omega t}\sum_{n=1}^{\infty} 2P_n, \tag{6.13}$$

and

$$\mathrm{P}(jk;\epsilon) = \frac{1}{2\pi}e^{j\omega t}\int_1^{\infty} e^{-jk\Theta} f'(\xi_0)\frac{\xi_0+1}{\xi_0-1}\,d\xi_0. \tag{6.14}$$

With that the constant γ_0 can be expressed in terms of Q and $\mathrm{P}(jk;\epsilon)$, namely

$$\gamma_0 = -Q/\mathrm{P}(jk;\epsilon).$$

Substituting this result for γ_0 into equation (6.8), it follows that

$$\hat{F}_2(\zeta,t) = -\frac{i}{2\pi}\frac{Q}{\mathrm{P}(jk;\epsilon)}e^{j\omega t}\int_1^{\infty} e^{-jk\Theta} f'(\xi_0)\log\frac{\zeta-\xi_0}{\zeta-\xi_0^{-1}}\,d\xi_0. \tag{6.15}$$

Recall that Q can be determined from the boundary condition, i.e. it depends upon the displacement function, the steady-state velocity potential, and the

mapping function; and that $P(jk;\epsilon)$ depends upon the mapping function and the reduced frequency. These functions and quantities are assumed to be known. Thus, the total complex velocity potential function

$$\hat{F}(\zeta,t)=\hat{F}_0(\zeta)+\hat{F}_1(\zeta,t)+\hat{F}_2(\zeta,t) \tag{6.16}$$

is known for any prescribed flapping function and thickness parameter.

7. Pressure distribution resulting from source potential

The unsteady pressure distribution resulting from the source potential can be found by inserting the source potential function (5.18) into the linearized Bernoulli equation. Thus, applying equation (4.4), this pressure becomes

$$\Pi_1(\vartheta,t)=-\mathrm{Re}_i\rho\left[\frac{\partial}{\partial t}+\frac{\overline{F_0'(e^{i\vartheta})}}{|f'(e^{i\vartheta})|^2}\frac{\partial}{\partial\zeta}\right]\frac{U}{2\pi}e^{j\omega t}\int_0^{2\pi}G(\varphi)\log(\zeta-e^{i\varphi})^2\,d\varphi\Big|_{\zeta=e^{i\vartheta}}. \tag{7.1}$$

Combining equation (5.1) with this expression, performing the indicated differentiation, and observing that the Re_i operator and the integral operator are interchangeable, we are led to the result that

$$\Pi_1(\vartheta,t)=-\rho\frac{U^2}{2\pi}e^{j\omega t}\int_0^{2\pi}G(\varphi)\left\{\sigma\,\mathrm{Re}_i\log(e^{i\vartheta}-e^{i\varphi})^2-\frac{\sin\vartheta}{|f'(e^{i\vartheta})|^2}\mathrm{Re}_i\left(\frac{2ie^{i\vartheta}}{e^{i\vartheta}-e^{i\varphi}}\right)\right\}d\varphi, \tag{7.2}$$

where

$$\sigma=j\omega/U.$$

After some algebraic and trigonometric manipulations, this last result can be simplified to read

$$\Pi_1(\vartheta,t)=-\rho\frac{U^2}{2\pi}e^{j\omega t}\int_0^{2\pi}G(\varphi)\left\{\sigma\log\left(2\sin\frac{\vartheta-\varphi}{2}\right)^2+\frac{\sin\vartheta}{|f'(e^{i\vartheta})|^2}\cot\frac{\varphi-\vartheta}{2}\right\}d\varphi. \tag{7.3}$$

Recalling that $G(\varphi)$ is an odd function and that the integrand in equation (7.3) is periodic in 2π this formula can be simplified in a straightforward manner to

$$\Pi_1(\vartheta,t)=-\rho\frac{U^2}{2\pi}e^{j\omega t}\left\{\int_0^{\pi}G(\varphi)\left[\sigma\log\frac{1-\cos(\vartheta-\varphi)}{1-\cos(\vartheta+\varphi)}+2\frac{\sin\vartheta}{|f'(e^{i\vartheta})|^2}\frac{\sin\vartheta}{\cos\vartheta-\cos\varphi}\right]d\varphi\right\}. \tag{7.4}$$

Substituting the trigonometric series for $G(\varphi)$ given by equation (5.16) into equation (7.4) and performing the indicated integration, there follows, by using the relations

$$\frac{1}{\pi}\int_0^{\pi}\frac{\sin\varphi\sin n\varphi}{\cos\vartheta-\cos\varphi}d\varphi=\cos n\vartheta$$

and

$$\frac{1}{\pi}\int_0^{\pi}\log\frac{1-\cos(\vartheta-\varphi)}{1-\cos(\vartheta+\varphi)}\sin n\varphi\,d\varphi=-\frac{2}{n}\sin n\vartheta,$$

the result

$$\Pi_1(\vartheta,t)=2\rho U^2e^{j\omega t}\sum_{n=1}^{\infty}P_n\left[\sigma\frac{\sin n\vartheta}{n}-\frac{\sin\vartheta}{|f'(e^{i\vartheta})|^2}\cos n\vartheta\right]. \tag{7.5}$$

To this must be added the pressure distribution resulting from the vortices in the fish's wake.

8. Pressure distribution resulting from vortex potential

To determine the pressure distribution on the surface of the profile due to vortices in the wake, it is convenient to compute the pressure $d\Pi_2$ due to a single vortex pair of equal strength and opposite orientation located at ξ_0 and ξ_0^{-1} in the ζ-plane or the corresponding points in the profile or z-plane. The complex velocity potential of this pair was found to be

$$d\hat{F}_2(\zeta, t) = \frac{i}{2\pi} d\hat{\Gamma} \log \frac{\zeta - \xi_0}{\zeta - \xi_0^{-1}}. \tag{8.1}$$

According to Helmholtz's law of persistence of vorticity following a fluid particle, the strength $d\hat{\Gamma}$ is constant referred to a co-ordinate system moving with the fluid particle. Here it is assumed that the velocity of a fluid particle in the wake is equal to the steady-state local velocity, which is, of course, only approximately true. The wake streamline coincides with the positive x-axis in the profile plane. Therefore

$$\frac{\partial}{\partial t}(dF_2) = \frac{dx_0}{dt} \frac{\partial \xi_0}{\partial x_0} \frac{\partial}{\partial \xi_0}(d\hat{F}_2), \tag{8.2}$$

where x_0 is the co-ordinate of the vortex element in the profile plane.

From equation (4.4) the unsteady pressure due to this vortex pair is

$$d\Pi_2(\vartheta, t) = -\mathrm{Re}_i \rho \left[\frac{dx_0}{dt} \frac{\partial \xi_0}{\partial x_0} \frac{\partial}{\partial \xi_0} + \frac{\overline{F_0'(e^{i\vartheta})}}{|f'(e^{i\vartheta})|^2} \frac{\partial}{\partial \zeta} \right] d\hat{F}_2(\zeta, t)|_{\zeta = e^{i\vartheta}}, \tag{8.3}$$

where

$$\frac{dx_0}{dt} = \overline{F_0'(x_0)} = \overline{F'(\xi_0)/f'(\xi_0)} \tag{8.4}$$

is the local velocity of the vortex element $d\Gamma$ along the wake streamline in the profile plane.

Combining equations (5.1) and (8.4) with equation (8.3) and performing the indicated operations leads to the result

$$d\Pi_2(\vartheta, t) = \frac{\rho}{2\pi} d\hat{\Gamma} \left[\frac{\overline{F_0'(\xi_0)}}{|f'(\xi_0)|^2} \frac{2 \sin \vartheta}{\xi_0^2 + 1 - 2\xi_0 \cos \vartheta} + U \frac{\sin \vartheta}{|f'(e^{i\vartheta})|^2} \frac{\xi_0^2 - 1}{\xi_0^2 + 1 - 2\xi_0 \cos \vartheta} \right]. \tag{8.5}$$

To determine the effect of the entire wake vortex sheet, we replace the vortex element $d\hat{\Gamma}$ by

$$d\hat{\Gamma} = \hat{\gamma}_w d\xi_0 \tag{8.6}$$

and integrate over the entire wake. Thus,

$$\Pi_2(\vartheta, t) = \frac{\rho}{2\pi} \int_1^\infty \left[\frac{\overline{F_0'(\xi_0)}}{|f'(\xi_0)|^2} \frac{2 \sin \vartheta}{\xi_0^2 + 1 - 2\xi_0 \cos \vartheta} + U \frac{\sin \vartheta}{|f'(e^{i\vartheta})|^2} \frac{\xi_0^2 - 1}{\xi_0^2 + 1 - 2\xi_0 \cos \vartheta} \right] \hat{\gamma}_w(\xi_0, t) \, d\xi_0. \tag{8.7}$$

Employing the results as given by equations (6.5), and (6.6) this last expression can be written as

$$\Pi_2(\vartheta, t) = \frac{\rho}{2\pi} \gamma_0 e^{j\omega t} \int_1^\infty \left[\frac{\overline{F_0'(\xi_0)}}{|f'(\xi_0)|^2} \frac{2 \sin \vartheta}{\xi_0^2 + 1 - 2\xi_0 \cos \vartheta} + U \frac{\sin \vartheta}{|f'(e^{i\vartheta})|^2} \frac{\xi_0^2 - 1}{\xi_0^2 + 1 - 2\xi_0 \cos \vartheta} \right] f'(\xi_0) \, e^{-jk\Theta} \, d\xi_0. \tag{8.8}$$

Eliminating the constant γ_0 by way of equation (6.12) the unsteady pressure as a result of the wake vortices becomes

$$\Pi_2(\vartheta, t) = -\rho Q T(\vartheta, jk;\, \epsilon), \tag{8.9}$$

where

$$T(\vartheta, jk;\, \epsilon) = \frac{\int_1^\infty \left[\frac{\overline{F_0'(\xi_0)}}{|f'(\xi_0)|^2}\frac{2\sin\vartheta}{\xi_0^2+1-2\xi_0\cos\vartheta} + U\frac{\sin\vartheta}{|f'(e^{i\vartheta})|^2}\frac{\xi_0^2-1}{\xi_0^2+1-2\xi_0\cos\vartheta}\right] f'(\xi_0)\, e^{-jk\Theta}\, d\xi_0}{\int_1^\infty \frac{\xi_0+1}{\xi_0-1}\, e^{-jk\Theta} f'(\xi_0)\, d\xi_0}. \tag{8.10}$$

Adding now equations (7.5) and (8.9) gives the desired unsteady pressure distribution as

$$\Pi(\vartheta, t) = 2\rho U^2 e^{j\omega t} \sum_{n=1}^{\infty} P_n \left[\sigma\frac{\sin n\vartheta}{n} - \frac{\sin\vartheta}{|f'(e^{i\vartheta})|^2}\cos n\vartheta + \frac{T(\vartheta, jk;\, \epsilon)}{U}\right], \tag{8.11}$$

where the series for Q given by equation (6.13) has been employed. For the special case of a flat deformable plate of infinitesimal thickness, the parameter ϵ vanishes and the equation (8.11) reduces to

$$\Pi(\vartheta, t) = \frac{\rho U^2}{\pi} e^{j\omega t} \int_0^\pi \left\{\frac{\sigma}{2}\log\frac{1-\cos(\vartheta+\varphi)}{1-\cos(\vartheta-\varphi)} + \frac{1}{\sin\vartheta}\frac{\sin\varphi}{\cos\varphi-\cos\vartheta} + \cot\frac{\varphi}{2}\left[\cot\vartheta + \frac{1-\cos\vartheta}{\sin\vartheta}\,\mathfrak{C}(k)\right]\right\} G(\varphi)\, d\varphi.$$

With some manipulations this can be expressed in identical form with that given by Siekmann (1962). The function $\mathfrak{C}(k)$ is the so-called Theodorsen function, defined by

$$\mathfrak{C}(k) = \frac{\int_1^\infty \frac{x_0}{(x_0^2-1)^{\frac{1}{2}}}\, e^{-jkx_0}\, dx_0}{\int_1^\infty \frac{x_0+1}{(x_0^2-1)^{\frac{1}{2}}}\, e^{-jkx_0}\, dx_0} = \frac{H_1^{(2)}(k)}{H_1^{(2)}(k)+jH_0^{(2)}(k)} = \mathfrak{F}(k)+j\mathfrak{G}(k)$$

where $H_0^{(2)}(k)$ and $H_1^{(2)}(k)$ are Hankel functions of the second kind of order zero and one, respectively.

9. Lift, moment and thrust

Equation (8.11) expresses the unsteady pressure distribution along the surface of the profile. The forces acting on the profile can be found by integrating this pressure distribution along the contour $\mathfrak{k}^*$ of the base profile. In complex notation the force function is

$$F_x - iF_y = -i\oint_{\mathfrak{k}^*} \Pi(\vartheta, t)\, d\bar{z}_0, \tag{9.1}$$

where $d\bar{z}_0 = d\bar{z}_{0P}$ gives

$$d\bar{z}_0 = \frac{d\bar{z}_0}{d\vartheta}\, d\vartheta = \frac{d\overline{f(e^{i\vartheta})}}{d\vartheta}\, d\vartheta.$$

Thus we obtain for the lift

$$L = F_y = \mathrm{Re}_i \int_0^{2\pi} \Pi \frac{d\bar{f}}{d\vartheta} d\vartheta. \tag{9.2}$$

The moment about the origin of the z-plane due to the force elements acting on an arc element ds is given by

$$dM = \Pi(\vartheta, t)(x\,dx + y\,dy) = \mathrm{Re}_i(\Pi z_0 d\bar{z}_0)$$

taken in the counter-clockwise sense. Thus the total moment is found to be

$$M = \mathrm{Re}_i \int_0^{2\pi} \Pi(\vartheta, t) f(e^{i\vartheta}) \frac{d\bar{f}}{d\vartheta} d\vartheta. \tag{9.3}$$

It is to be noted that the equations for lift and moment neglect the change in shape of the profile since it is assumed that the pressure acts in a direction normal to the surface of the base profile.

In order to calculate the x-component of the resultant hydrodynamic force acting on the plate, the change in shape of the profile must be taken into consideration. As shown by Wu (1961) and Siekmann (1962), the important fact here is that non-linear terms are involved and, as such, there are mixed terms involving the time imaginary unit j. Therefore, the real part with respect to time imaginary unit must be taken for physical interpretation. The hydrodynamic force in question can be determined from the equation

$$d(F_x - iF_y) = -i\Pi(\vartheta, t)\, d\bar{z}_P.$$

Now for the differential $d\bar{z}_P$ we obtain by applying equation (5.2) and (5.11) the expression

$$d\bar{z}_P = d\overline{f(e^{i\vartheta})} - i e^{j\omega t} dH_1^*(\vartheta). \tag{9.4}$$

It is to be noted that the coefficients B_n in equation (5.12) are generally complex in the time imaginary unit j. Thus, from equations (9.1) and (9.4), the x-component of the hydrodynamic force becomes

$$F_x = \mathrm{Re}_i \left\{ -i \int_0^{2\pi} \mathrm{Re}_j\, \Pi(\vartheta, t) \left[\frac{d\bar{f}}{d\vartheta} - i\, \mathrm{Re}_j e^{j\omega t} \frac{dH_1^*(\vartheta)}{d\vartheta} \right] d\vartheta \right\}, \tag{9.5}$$

where Re_j is the 'real part' operator with respect to the time imaginary unit j. A positive F_x will indicate a net drag.

10. Application of the theory to a symmetric Joukowski profile with a linearized thickness parameter

For profiles of small finite thickness, as are considered here, we linearize in the small thickness parameter all functions containing this parameter.

First of all we want to calculate the 'downwash' velocity for any given flapping function. The downwash velocity on the boundary of the circle is determined by equation (5.14). Then the corresponding downwash velocity on the base profile is given by

$$q_n(\vartheta, t) = \frac{\hat{q}_r(\vartheta, t)}{f'(e^{i\vartheta})}.$$

We recall that the function $G(\vartheta)$ occurring in equation (5.14) is given by equation (5.15). Taking now the derivatives of equation (3.8) yields

$$f'(e^{i\vartheta}) = \tfrac{1}{2}[1 - e^{-2i\vartheta} + 2\epsilon(e^{-2i\vartheta} - e^{-3i\vartheta})].$$

Separating the real and imaginary parts and changing i to $-i$ the foregoing equation becomes

$$f'(e^{i\vartheta}) = \tfrac{1}{2}(\nu_1 + i\nu_2),$$

where

$$\nu_1 = 1 - \cos 2\vartheta + 2\epsilon(\cos 2\vartheta - \cos 3\vartheta),$$

$$\nu_2 = -\sin 2\vartheta + 2\epsilon(\sin 2\vartheta - \sin 3\vartheta).$$

After some algebraic and trigonometric manipulations we find for $[f'(e^{i\vartheta})]^{-1}$ the expression

$$[f'(e^{i\vartheta})]^{-1} = \frac{\nu_3 + i\nu_4}{2(1-2\epsilon)\sin^2\vartheta},$$

with

$$\nu_3 = 1 - 2\epsilon\cos\vartheta - (1-2\epsilon)\cos 2\vartheta,$$

$$\nu_4 = 2\epsilon\sin\vartheta - (1-2\epsilon)\sin 2\vartheta.$$

Quadratic terms in ϵ have been neglected. Substituting now the corresponding formulae into equation (5.15) leads to

$$G(\vartheta) = -\left[\tfrac{1}{2}\sigma(\nu_2\cos\vartheta - \nu_1\sin\vartheta)\,H_1^*(\vartheta) - \frac{\nu_4\cos\vartheta - \nu_3\sin\vartheta}{2(1-2\epsilon)\sin\vartheta}\,\frac{dH_1^*(\vartheta)}{d\vartheta}\right],$$

which can be simplified to read

$$G(\vartheta) = \sigma[(1-\epsilon)\sin\vartheta + \epsilon\sin 2\vartheta]\,H_1^*(\vartheta) + \left[-\frac{1+\epsilon}{1-2\epsilon} + \frac{2\epsilon}{1-2\epsilon}\cos\vartheta\right]\frac{dH_1^*(\vartheta)}{d\vartheta}. \tag{10.1}$$

It is expedient at this point to introduce a new function $g(\vartheta)$ defined by

$$g(\vartheta) = \frac{G(\vartheta)}{\sin\vartheta} = 2\sum_{n=1}^{\infty} P_n\frac{\sin n\vartheta}{\sin\vartheta} = A_0 + 2\sum_{n=1}^{\infty} A_n\cos n\vartheta, \tag{10.2}$$

where the Fourier coefficients are related according to

$$A_{n-1} - A_{n+1} = 2P_n \quad (n = 1, 2, 3, \ldots). \tag{10.3}$$

Combining equations (10.1) and (10.2), it follows that

$$g(\vartheta) = \sigma(1 - \epsilon + 2\epsilon\cos\vartheta)\,H_1^*(\vartheta) + \left[-\frac{1+\epsilon}{1-2\epsilon} + \frac{2\epsilon}{1-2\epsilon}\cos\vartheta\right]\frac{1}{\sin\vartheta}\,\frac{dH_1^*(\vartheta)}{d\vartheta}. \tag{10.4}$$

If we set

$$\frac{1}{\sin\vartheta}\,\frac{dH_1^*(\vartheta)}{d\vartheta} = -2\sum_{n=1}^{\infty} nB_n\frac{\sin n\vartheta}{\sin\vartheta} = C_0 + 2\sum_{n=1}^{\infty} C_n\cos n\vartheta, \tag{10.5}$$

where the recurrence relation for the Fourier coefficients is given by

$$C_{n-1} - C_{n+1} = -2nB_n \quad (n \geqslant 1), \tag{10.6}$$

then with some straightforward calculations we get

$$\left.\begin{aligned} A_0 &= \sigma[(1-\epsilon)B_0 + 2\epsilon B_1] - \frac{1+\epsilon}{1-2\epsilon}C_0 + \frac{2\epsilon}{1-2\epsilon}C_1, \\ A_n &= \sigma[(1-\epsilon)B_n + \epsilon(B_{n+1} + B_{n-1})] + \frac{1+\epsilon}{1-2\epsilon}C_n + \frac{\epsilon}{1-2\epsilon}(C_{n+1} + C_{n-1}) \quad (n \geqslant 1). \end{aligned}\right\} \tag{10.7}$$

It should be noted that the trigonometric series in which the coefficients are the A_n's is related to the downwash velocity on the surface of the profile, whereas the series containing the B_n's and the C_n's are associated with the flapping and the displacement of the fish, respectively. Hence, equation (10.7) relates the downwash velocity in terms of the displacement and displacement rate of the fish.

11. Pressure distribution approximation

In order to determine the pressure distribution we first approximate the difficult wake effect as contained in the function $T(\vartheta, jk; \epsilon)$ given by equation (8.10). It is seen that the velocity of a fluid particle emanating from the sharp tail is reduced somewhat from the free stream velocity. This slowing-up effect is greatest near the tail. Thus, while the wake vortices far downstream convect with a velocity U, those near the trailing edge connect with a smaller velocity. Since such near vortices are likely to have a more pronounced effect on the body, a reasonable approximate way of dealing with them is to replace the potential $\hat{F}_2$ as given in equation (6.15) by what it would be for a thin plate hydrofoil immersed in a stream of slightly reduced velocity. Accordingly, for determining the effect of the wake on the pressure distribution, we represent the profile by its mean chord line immersed in a uniform flow with a velocity δU, where δ represents the slowing-up effect due to thickness. The parameter δ is related to the thickness parameter ϵ. For the special case of vanishing thickness ($\epsilon = 0$) we have $\delta = 1$. We determine this relationship by requiring that the time-dependent pressure vanishes at the tail for all time.

From equation (3.8) it follows that the actual chord length of the stretched-straight profile is given by $|x_T - x_L| = 2(1-\epsilon)$.

This actual chord line can be mapped on to the unit circle by the transformation

$$z = f(\zeta) = \lambda(\zeta + \zeta^{-1} + \beta), \tag{11.1}$$

where the values of λ and β are found to be

$$\lambda = \tfrac{1}{2}(1-\epsilon), \quad \beta = (1-\epsilon)^{-1}(2-\epsilon) - 2.$$

In this flow field the steady-state potential becomes

$$\hat{F}_0(\zeta) = \tfrac{1}{2}\delta U(\zeta + \zeta^{-1}). \tag{11.2}$$

It further turns out from equation (6.7) that

$$\Theta = \int_1^{\xi_0} \frac{\lambda^2(1-\xi_0^{-2})^2}{\frac{1}{2}\delta(1-\xi_0^{-2})}\, d\xi_0 = \frac{2\lambda^2}{\delta}\left(\xi_0 + \frac{1}{\xi_0} - 2\right). \tag{11.3}$$

In establishing this formula the relation

$$f'(\xi_0) = \lambda(1-\xi_0^{-2})$$

resulting from equation (10.1) was used. We now introduce a variable χ defined by

$$\xi_0 = e^{\chi}; \tag{11.4}$$

with this we obtain

$$\overline{dF_0(\chi)/d\chi} = \overline{F_0'(\chi)} = \delta U e^{-\chi}\sinh\chi,$$

$$df(\chi)/d\chi = f'(\chi) = 2\lambda e^{-\chi}\sinh\chi,$$

and

$$\Theta = 4\lambda^2\delta^{-1}(\cosh\chi - 1).$$

Substituting the above results into equation (8.10) we obtain the expression for the wake function $T(\vartheta, jk;\ \epsilon)$ in terms of the new variable as

$$T(\vartheta, jk;\ \epsilon) = \frac{\dfrac{\delta U}{4\lambda^2}\displaystyle\int_0^\infty \left[\frac{2e^\chi\sin\vartheta}{e^{2\chi}+1-2e^\chi\cos\vartheta} + \frac{\sinh\chi}{\sin\vartheta}\frac{e^{2\chi}-1}{e^{2\chi}+1-2e^\chi\cos\vartheta}\right] e^{-j\Lambda k\cosh\chi}\,d\chi}{\displaystyle\int_0^\infty \frac{e^\chi+1}{e^\chi-1}\sinh\chi\, e^{-j\Lambda k\cosh\chi}\,d\chi}, \tag{11.5}$$

where

$$\Lambda = 4\lambda^2/\delta.$$

After some straightforward calculations, this expression can be written as

$$T(\vartheta, jk;\ \epsilon) = \frac{U}{\Lambda\sin\vartheta}\frac{\displaystyle\int_0^\infty (\cosh\chi + \cos\vartheta)\, e^{-j\Lambda k\cosh\chi}\,d\chi}{\displaystyle\int_0^\infty (\cosh\chi + 1)\, e^{-j\Lambda k\cosh\chi}\,d\chi}. \tag{11.6}$$

Now from the theory of Bessel functions (Watson 1948) we know that

$$K_n(z) = \int_0^\infty e^{-z\cosh\chi}\cosh n\chi\, d\chi, \tag{11.7}$$

where $K_n(z)$ is the nth-order Bessel function of the second kind. This relation is valid if $|\arg z| < \frac{1}{2}\pi$, which requires that $\mathrm{Re}_j z > 0$.

Thus, combining equations (11.6) and (11.7) we are led to the result

$$T(\vartheta, jk;\ \epsilon) = \frac{U}{\Lambda\sin\vartheta}\left[(1-\cos\vartheta)\frac{K_1(j\Lambda k)}{K_1(j\Lambda k)+K_0(j\Lambda k)} + \cos\vartheta\right]. \tag{11.8}$$

The ratio containing the Bessel functions in the above expression is the Theodorsen function $\mathfrak{C}(\Lambda k)$ (Theodorsen 1934). Employing the relation (Watson 1948)

$$K_n(j\Lambda k) = \tfrac{1}{2}\pi j^{-n-1}H_n^{(2)}(\Lambda k), \tag{11.9}$$

where $H_n^{(2)}(k)$ are Hankel functions of the second kind and of order n, it follows that

$$\mathfrak{C}(\Lambda k) = \frac{K_1(j\Lambda k)}{K_1(j\Lambda k)+K_0(j\Lambda k)} = \frac{H_1^{(2)}(\Lambda k)}{H_1^{(2)}(\Lambda k)+jH_0^{(2)}(\Lambda k)}. \tag{11.10}$$

In the development of equation (11.10) we imposed the condition that

$$\mathrm{Re}_j z = \mathrm{Re}_j(j\Lambda k) > 0.$$

However, according to Luke & Dengler (1951) this equation has no need for such a restriction and therefore, by analytic continuation, one can argue that this formula holds for all $\mathrm{Re}_j(j\Lambda k)$. In the present case we have $\mathrm{Re}_j(j\Lambda k) = 0$.

Combining equations (11.8) through (11.10) with equation (8.11), the unsteady pressure distribution becomes

$$\Pi(\vartheta,t) = 2\rho U^2 e^{j\omega t} \sum_{n=1}^{\infty} P_n \left\{ \sigma \frac{\sin n\vartheta}{n} - \frac{\sin\vartheta}{|f'(e^{i\vartheta})|^2} \cos n\vartheta + \frac{1}{\Lambda \sin\vartheta} [\mathfrak{C}(\Lambda k) + (1 - \mathfrak{C}(\Lambda k)) \cos\vartheta] \right\}. \quad (11.11)$$

From equation (3.7) it follows that

$$\frac{1}{|f'(e^{i\vartheta})|^2} = \left\{ \frac{1}{2}\left[1 - \left(\frac{1-\epsilon}{e^{i\vartheta}-\epsilon}\right)^2\right] \frac{1}{2}\left[1 - \left(\frac{1-\epsilon}{e^{-i\vartheta}-\epsilon}\right)^2\right] \right\}^{-1}. \quad (11.12)$$

After some straightforward calculations and linearizing in ϵ, equation (11.12) reduces to

$$\frac{1}{|f'(e^{i\vartheta})|^2} = \frac{1 - 4\epsilon\cos\vartheta}{(1-2\epsilon)\sin^2\vartheta}. \quad (11.13)$$

Combining equation (11.11) and (11.13), we obtain

$$\Pi(\vartheta,t) = 2\rho U^2 e^{j\omega t} \sum_{n=1}^{\infty} P_n \left\{ \sigma \frac{\sin n\vartheta}{n} - \frac{1-4\epsilon\cos\vartheta}{1-2\epsilon} \frac{\cos n\vartheta}{\sin\vartheta} + \frac{1}{\Lambda \sin\vartheta} [\mathfrak{C}(\Lambda k) + (1 - \mathfrak{C}(\Lambda k)) \cos\vartheta] \right\}. \quad (11.14)$$

It can be seen from this expression that the unsteady pressure possesses a singularity at the tail where $\vartheta = 0$ and at the nose where $\vartheta = \pi$. The singularity at the tail is removed by satisfying the condition

$$\Pi(0,t) = \lim_{\vartheta\to 0} \left[-\frac{1-4\epsilon}{1-2\epsilon} + \frac{1}{\Lambda} \right] \frac{1}{\sin\vartheta} = 0. \quad (11.15)$$

This can be satisfied for all time only if

$$(1-2\epsilon)^{-1}(1-4\epsilon) = \Lambda^{-1}.$$

The singularity at $\vartheta = \pi$ produces a concentrated force at the nose, the so-called suction force arrived at in airfoil theory, which must be added to the hydrodynamic force computed by integrating the pressure distribution around the profile.

For the subsequent calculations, it is convenient to express the unsteady pressure distribution in a Glauert trigonometric series as

$$\Pi(\vartheta,t) = \rho U^2 e^{j\omega t} \left(a_0 \tan\tfrac{1}{2}\vartheta + 2 \sum_{n=1}^{\infty} a_n \sin n\vartheta \right) \quad (11.16)$$

where the coefficients after some laborious manipulations are found to be

$$\left.\begin{aligned} a_0 &= r_0 - 2\epsilon(r_0 + 2A_1 - 2A_0), \\ a_n &= A_n + \tfrac{1}{2}\sigma \frac{A_{n-1} - A_{n+1}}{n} + 2\epsilon(A_n - A_{n-1} - A_{n+1}) \quad (n \geqslant 1), \end{aligned}\right\} \quad (11.16a)$$

with

$$r_0 = (A_0 + A_1)\,\mathfrak{C}(\Lambda k) - A_1. \quad (11.16b)$$

12. Calculation of the lift and moment

With the pressure distribution known (equation (11.16)), the lift can be calculated from equation (9.2) as

$$L = \mathrm{Re}_i \int_0^{2\pi} \Pi(\vartheta, t)\, d\bar{f},$$

where the differential $d\bar{f}$ must be found from the mapping function (equation (3.8)). We obtain

$$d\bar{f} = [-(1-\epsilon)\sin\vartheta - \epsilon\sin 2\vartheta - i\epsilon(\cos\vartheta - \cos 2\vartheta)]\, d\vartheta.$$

Since $\Pi(\vartheta, t)$ is real with respect to the space imaginary unit i, the operator Re_i and the integral operator commute. Thus, carrying out the indicated operation we arrive at

$$L = -2\pi\rho U^2 e^{j\omega t}[(1-2\epsilon)\, a_0 + (1-\epsilon)\, a_1 + \epsilon a_2],$$

or by means of equations (11.16),

$$\begin{aligned} L = -2\pi\rho U^2 e^{j\omega t}\Big\{ & (A_0 + A_1)(1-4\epsilon)\,\mathfrak{C}(\Lambda k) - A_1 + 4\epsilon A_0 \\ & + (1-\epsilon)\left[\frac{A_1}{1-2\epsilon} + \sigma\frac{A_0 - A_2}{2} - 2\epsilon\frac{A_0 + A_2}{1-2\epsilon}\right] \\ & + \epsilon\left[\frac{A_2}{1-2\epsilon} + \sigma\frac{A_1 - A_3}{2} - 2\epsilon\frac{A_1 + A_3}{1-2\epsilon}\right]\Big\}. \end{aligned} \tag{12.1}$$

For the case of a flat plate of zero thickness ($\epsilon = 0$), the lift becomes

$$L = -2\pi\rho U^2 e^{j\omega t}\left[(A_0 + A_1)\,\mathfrak{C}(\Lambda k) + \sigma\frac{A_0 - A_2}{2}\right],$$

where $\Lambda = 1$. This is in agreement with the result of Siekmann (1962). In making a comparison between this work and that of Siekmann it must be observed that

$$A_n = (-1)^n A_n^*,$$

where the coefficients A_n^* correspond to Siekmann's coefficients for the 'downwash'. The difference in signs arises from the fact that Siekmann employs a pressure difference across the plate of $\Delta p = (p^- - p^+)$ to determine the lift, whereas in this work the analogous pressure difference is $\Delta p = (p^+ - p^-)$.

The moment about the origin of the forces acting on the profile is given, according to equation (9.3) by

$$M = \mathrm{Re}_i \int_0^{2\pi} \Pi(\vartheta, t) f(e^{i\vartheta})\, d\bar{f},$$

where the moment is positive if counter-clockwise (nose down).

Combining equation (3.7) with the expression for the differential $d\bar{f}$ yields, after linearizing the result in ϵ and straightforward calculations,

$$\mathrm{Re}_i[f(e^{i\vartheta})\, d\bar{f}] = \tfrac{1}{2}[-(1-2\epsilon)\sin 2\vartheta + 2\epsilon\cos\vartheta\sin 2\vartheta - \epsilon\sin\vartheta\cos 2\vartheta]\, d\vartheta.$$

Multiplication by $\Pi(\vartheta, t)$ and integration then leads to

$$M = \pi\rho U^2 e^{j\omega t}[(1-\epsilon)\, a_0 - (1-2\epsilon)\, a_2 + \epsilon(a_1 + a_3)],$$

or, in terms of the downwash velocity, the moment is finally found to be

$$M = \pi\rho U^2 e^{j\omega t}\Big\{(1-\epsilon)\,[r_0 - 2\epsilon(r_0 + 2A_1 - 2\dot{A}_0)]$$
$$-(1-2\epsilon)\left[A_2 + \sigma\frac{A_1 - A_3}{4} + 2\epsilon(A_2 - A_1 - A_3)\right]$$
$$+\epsilon\left[A_1 + A_3 + \sigma\left(\frac{A_0 - A_2}{2} + \frac{A_2 - A_4}{6}\right) + 2\epsilon(A_1 + A_3 - A_0 - 2A_2 - A_4)\right]\Big\}. \quad (12.2)$$

For the special case of a flat plate with vanishing thickness, the moment about the centre of the plate reduces to

$$M = \pi\rho U^2 e^{j\omega t}[(A_0 + A_1)\,\mathfrak{C}(k) - A_1 - A_2 - \tfrac{1}{4}\sigma(A_1 - A_3)].$$

This result is again in agreement with Siekmann (1962, equation (4.8)).

13. Calculation of the thrust

The net thrust or drag is given by the total hydrodynamic force acting on the plate in the x-direction. The x-component of the hydrodynamic force imposed on the profile by the pressure distribution is given by equation (9.5). Due to the singularity in the pressure at the nose, the force as given by equation (9.5) must be supplemented by the so-called suction force which is concentrated at the nose.

It is convenient for calculation purposes to decompose the thrust into three parts as follows

$$F_x = F_x^{(1)} + F_x^{(2)} + F_x^{(3)},$$

where

$$F_x^{(1)} = \mathrm{Re}_i\left\{-i\int_0^{2\pi} \mathrm{Re}_j\,\Pi(\vartheta, t)\frac{d\bar{f}}{d\vartheta}\,d\vartheta\right\},$$

$$F_x^{(2)} = \mathrm{Re}_i\left\{-i\int_0^{2\pi} \mathrm{Re}_j\,\Pi(\vartheta, t)\left[-i\,\mathrm{Re}_j e^{j\omega t}\frac{dH_1^*(\vartheta)}{d\vartheta}\right]d\vartheta\right\},$$

and $F_x^{(3)}$ is the suction force. The term $F_x^{(1)}$ represents the streamwise force computed by integrating the pressure distribution along the contour $\mathfrak{k}^*$ defined by the stretched-straight configuration of the profile, whereas the term $F_x^{(2)}$ represents the streamwise force computed by considering the displacement and the rate of displacement of the profile.

We define the following quantities:

$$\tilde{r}_0 = \tilde{r}_0' + j\tilde{r}_0'' = r_0 e^{j\omega t} = (r_0' + jr_0'')\,e^{j\omega t}, \quad (13.1a)$$
$$\tilde{a}_n = \tilde{a}_n' + j\tilde{a}_n'' = a_n e^{j\omega t} = (a_n' + ja_n'')\,e^{j\omega t}, \quad (13.1b)$$
$$\tilde{A}_n = \tilde{A}_n' + j\tilde{A}_n'' = A_n e^{j\omega t} = (A_n' + jA_n'')\,e^{j\omega t}, \quad (13.1c)$$
$$\tilde{B}_n = \tilde{B}_n' + j\tilde{B}_n'' = B_n e^{j\omega t} = (B_n' + jB_n'')\,e^{j\omega t}, \quad (13.1d)$$
$$\tilde{C}_n = \tilde{C}_n' + j\tilde{C}_n'' = C_n e^{j\omega t} = (C_n' + jC_n'')\,e^{j\omega t}, \quad (13.1e)$$

where for example

$$\tilde{a}_n' = a_n' \cos\omega t - a_n'' \sin\omega t, \quad (13.1f)$$
$$\tilde{a}_n'' = a_n'' \cos\omega t + a_n' \sin\omega t, \quad (13.1g)$$
etc.

Employing these results and equation (11.16), it follows first of all that

$$\mathrm{Re}_j \Pi(\vartheta, t) = \rho U^2 \left[\tilde{a}_0' \tan \tfrac{1}{2}\vartheta + 2 \sum_{n=1}^{\infty} \tilde{a}_n' \sin n\vartheta \right]. \tag{13.2}$$

Also from equations (5.12) and (13.1*d*) it can be shown that

$$\mathrm{Re}_j e^{j\omega t} \frac{dH_1^*(\vartheta)}{d\vartheta} = -2 \sum_{n=1}^{\infty} n \tilde{B}_n' \sin n\vartheta. \tag{13.3}$$

This last expression can be written in a more convenient form as

$$-2 \sum_{n=1}^{\infty} n \tilde{B}_n' \frac{\sin n\vartheta}{\sin \vartheta} \sin \vartheta = \left(\tilde{C}_0' + 2 \sum_{n=1}^{\infty} \tilde{C}_n' \cos n\vartheta \right) \sin \vartheta, \tag{13.4}$$

where the relationships between the B_n' and the C_n' are given in equation (10.6).

Substituting equation (13.2) into the expression for $F_x^{(1)}$ and applying the relation

$$\int_0^{2\pi} \sin n\vartheta \cos m\vartheta \, d\vartheta = 0$$

leads to the result that

$$F_x^{(1)} = -\epsilon \rho U^2 \tilde{a}_0' \oint_0^{2\pi} \tan \tfrac{1}{2}\vartheta (\cos \vartheta - \cos 2\vartheta) \, d\vartheta,$$

where the integral has to be taken as a Cauchy principal value. It can be shown that this integral vanishes, hence $F_x^{(1)} = 0$.

Next by substituting equations (13.2), (13.3) and (13.4) into the equation for $F_x^{(2)}$ and employing the integrals

$$\int_0^{2\pi} \tan \tfrac{1}{2}\vartheta \sin n\vartheta \, d\vartheta = (-1)^{n+1} 2\pi \quad (n \geqslant 1),$$

and

$$\int_0^{2\pi} \sin m\vartheta \sin n\vartheta \, d\vartheta = \begin{cases} \pi, & m = n, \\ 0, & m \neq n, \end{cases}$$

we obtain

$$F_x^{(2)} = -2\pi\rho U^2 \left[\tilde{a}_0' \sum_{n=1}^{\infty} (-1)^{n+1} (-2n\tilde{B}_n') - 2 \sum_{n=1}^{\infty} n \tilde{a}_n' \tilde{B}_n' \right]. \tag{13.5}$$

But, according to equation (10.6),

$$-2 \sum_{n=1}^{\infty} (-1)^{n+1} n \tilde{B}_n' = \tilde{C}_0' - \tilde{C}_1'.$$

Inserting this expression into equation (13.5) yields

$$F_x^{(2)} = -2\pi\rho U^2 \left[\tilde{a}_0' (\tilde{C}_0' - \tilde{C}_1') - 2 \sum_{n=1}^{\infty} n \tilde{a}_n' \tilde{B}_n' \right]. \tag{13.6}$$

To the above force must be added the concentrated force at the nose. Since the leading edge suction force arises from the singular pressure at the nose, it is necessary for its determination to take into account the non-linear terms in the expression for the pressure distribution in the neighbourhood of the leading edge. This can be accomplished most readily by considering the behaviour of the velocity as the leading edge is approached and by then employing the Blasius formula

to a small circle of radius δ_0 surrounding the nose. The velocity at the leading edge can be computed from the complex velocity potential by equation (3.9) as

$$\lim_{z\to x_L} w(z,t) = \lim_{\zeta\to -1} \overline{(\partial F/\partial\zeta)}\,(d\zeta/dz), \tag{13.7}$$

where

$$\overline{\partial F/\partial\zeta} = \hat{w}(\zeta,t)$$

is the complex velocity in the ζ-plane. Since $\hat{w}$ is bounded at the leading edge, this last expression can be written as

$$\lim_{z\to x_L} w(z,t) = \hat{w}(-1,t) \lim_{\zeta\to -1} d\zeta/dz. \tag{13.8}$$

But, from equation (3.7) it follows that

$$\zeta-\epsilon = z-\tfrac{1}{2}\epsilon+[(z-\tfrac{1}{2}\epsilon)^2+(1-\epsilon)^2]^{\frac{1}{2}}, \tag{13.9}$$

and, as $\zeta\to -1$, $z\to -1+\frac{3}{2}\epsilon$. Differentiation of equation (13.9) and carrying out the limiting process $\zeta\to -1$ yields

$$\lim_{\zeta\to -1} d\zeta/dz = \infty.$$

From these results it is seen that the velocity in the physical plane asymptotically approaches an infinite value as

$$\lim_{Z\to 0} w(\bar{z},t) = \hat{w}(-1,t) \lim_{Z\to 0}\left[\frac{\epsilon-1}{(\epsilon-1)^{\frac{1}{2}}}\frac{1}{(2Z)^{\frac{1}{2}}}+1\right], \tag{13.10}$$

where

$$Z = z+1-\tfrac{3}{2}\epsilon.$$

Now, Blasius's formula for the case of unsteady flow can be written as

$$F_x^{(3)}-iF_y^{(3)} = \tfrac{1}{2}i\rho\oint_{\mathfrak{k}_0}|w|^2\,dz - i\rho\oint_{\mathfrak{k}_0}\frac{\partial\Phi}{\partial t}\,d\bar{z}. \tag{13.11}$$

Here the contour $\mathfrak{k}_0$ is taken to be a small circle around the leading edge with a radius δ_0. Since the velocity potential Φ and its derivative $\partial\Phi/\partial t$ are bounded at the leading edge, the last contour integral in equation (13.11) vanishes.

Thus, combining equations (13.10) and (13.11), we obtain

$$F_x^{(3)}-iF_y^{(3)} = \tfrac{1}{2}i\rho\oint_{\mathfrak{k}_0}|\hat{w}(-1,t)|^2\left|\frac{\epsilon-1}{i(1-\epsilon)^{\frac{1}{2}}(2Z)^{\frac{1}{2}}}\right|^2 dz. \tag{13.12}$$

A small circle around the nose can be written in complex notation as

$$Z = \delta_0 e^{i\psi}. \tag{13.13}$$

Therefore

$$dz = dZ = \delta_0 i e^{i\psi}\,d\psi. \tag{13.14}$$

Hence, from these results we find that

$$F_x^{(3)}-iF_y^{(3)} = -\tfrac{1}{2}\pi\rho(1-\epsilon)\,|\hat{w}(-1,t)|^2. \tag{13.15}$$

Thus, $F_y^{(3)}$ vanishes and $F_x^{(3)}$ clearly represents a thrust term, i.e. a force directed along the negative x-axis.

To complete the calculation of the suction force, the complex velocity $\hat{w}(-1,t)$ in the ζ-plane must be found from the complex velocity potential

$\hat{F} = \hat{F}_0 + \hat{F}_1 + \hat{F}_2$. This can be done by considering separately the contributions to this velocity by each potential function and adding the results.

Thus, from equation (5.1) we obtain

$$\hat{w}_0(-1,t) = \overline{\left.\frac{dF_0(\zeta,t)}{d\zeta}\right|_{\zeta=-1}} = 0.$$

Equation (5.18) yields

$$\hat{w}_1(-1,t) = \overline{\left.\frac{\partial F_1(\zeta,t)}{\partial\zeta}\right|_{\zeta=-1}} = \frac{U}{2\pi} e^{j\omega t} \int_0^{2\pi} G(\varphi) \frac{2}{-1-e^{-i\varphi}} d\varphi.$$

Substituting the trigonometric series for $G(\varphi)$ and employing the integrals

$$\frac{1}{2\pi}\int_0^{2\pi} \sin n\varphi \, d\varphi = 0,$$

$$\frac{1}{2\pi}\int_0^{2\pi} \frac{\sin n\varphi \sin\varphi}{1+\cos\varphi} d\varphi = (-1)^{n+1} \quad (n \geqslant 1),$$

leads to

$$\hat{w}_1(-1,t) = -2iU e^{j\omega t} \sum_{n=1}^{\infty} (-1)^{n+1} P_n.$$

By applying the recurrence formula (10.3) we find that

$$\hat{w}_1(-1,t) = -iU e^{j\omega t}(A_0 - A_1). \tag{13.16}$$

The velocity $\hat{w}_2$ due to F_2 can be found from equation (6.15) to be

$$\hat{w}_2(-1,t) = \overline{\left.\frac{\partial F_2(\zeta,t)}{\partial\zeta}\right|_{\zeta=-1}} = \frac{i}{2\pi} \frac{Q}{\mathrm{P}(jk;\epsilon)} e^{j\omega t} \int_1^{\infty} \frac{\xi_0 - 1}{\xi_0 + 1} f'(\xi_0) e^{-jk\Theta} d\xi_0.$$

Inserting the expressing for $\mathrm{P}(jk;\epsilon)$ and substituting the approximate expressions derived earlier we find

$$\hat{w}_2(-1,t) = iQ \frac{K_1(j\Lambda k) - K_0(j\Lambda k)}{K_1(j\Lambda k) + K_0(j\Lambda k)}.$$

Combining now the formula for Q (equation 6.13) and the recurrence relation given by equation (10.3) it follows after some simplifications that

$$\hat{w}_2(-1,t) = -iU e^{j\omega t}(A_0 + A_1)[2\mathfrak{C}(\Lambda k) - 1]. \tag{13.17}$$

Hence according to equations (13.16) and (13.17) the velocity at the leading edge in the ζ-plane is

$$\hat{w}(-1,t) = -2iU e^{j\omega t}[(A_0 + A_1)\mathfrak{C}(\Lambda k) - A_1].$$

It then follows that the suction force becomes

$$F_x^{(3)} = -2\pi\rho U^2(1-\epsilon)(\tilde{r}_0')^2, \tag{13.18}$$

where

$$\tilde{r}_0' = (\tilde{A}_0 + \tilde{A}_1)\mathfrak{F}(\Lambda k) - (\tilde{A}_0'' + \tilde{A}_1'')\mathfrak{G}(\Lambda k) - \tilde{A}_1'.$$

Finally, by adding the results given in equations (13.6) and (13.18), the net thrust becomes

$$F_x = -(F_x^{(2)} + F_x^{(3)}) = 2\pi\rho U^2 \left[\tilde{a}_0'(\tilde{C}_0' - \tilde{C}_1') - 2\sum_{n=1}^{\infty} n\tilde{a}_n' \tilde{B}_n' + (1-\epsilon)(\tilde{r}_0')^2\right]. \tag{13.19}$$

From equations (11.16) and (13.1), we eliminate the $\tilde{a}'_n$ in equation (13.19). This gives for the thrust the formula

$$F_x = 2\pi\rho U^2 \Big\{ (\tilde{r}'_0 + \tilde{C}'_0)(\tilde{r}'_0 - \tilde{C}'_1) + k^2 \tilde{B}'_0 \tilde{B}'_1 + 4k \sum_{n=1}^{\infty} n \tilde{B}'_n \tilde{B}''_n$$
$$- \epsilon [2(\tilde{r}'_0 + 2\tilde{A}'_1 - 2\tilde{A}'_0)(\tilde{C}'_0 - \tilde{C}'_1) + 3(\tilde{C}'_0 \tilde{C}'_1 - \tilde{C}'_0 \tilde{C}'_0 + \tilde{C}'_1 \tilde{C}'_1) + (\tilde{r}'_0)^2]$$
$$- \epsilon \Big[k^2 (\tilde{B}'_0 \tilde{B}'_1 - \tilde{B}'_1 \tilde{B}'_1 - \tilde{B}'_0 \tilde{B}'_2) + k \sum_{n=1}^{\infty} n (\tilde{B}''_{n-1} + \tilde{B}''_{n+1}) \tilde{B}'_n$$
$$+ k \sum_{n=1}^{\infty} \frac{1}{2n} (\tilde{C}''_{|n-2|} - \tilde{C}''_{n+2})(\tilde{C}'_{n-1} - \tilde{C}'_{n+1}) \Big] \Big\}. \tag{13.20}$$

For the case of an infinitely thin plate the thrust reduces to

$$F_x = 2\pi\rho U^2 \Big[(\tilde{r}'_0 + \tilde{C}'_0)(\tilde{r}'_0 - \tilde{C}'_0) + k^2 \tilde{B}'_0 \tilde{B}'_1 + 4k \sum_{n=1}^{\infty} n \tilde{B}'_n \tilde{B}''_n \Big].$$

Now we can obtain easily that

$$\tilde{a}'_0 = \tilde{r}'_0 - 2\epsilon(\tilde{r}'_0 - 2\tilde{A}'_0 + 2\tilde{A}'_1).$$

According to this relation it is seen that $\tilde{r}'_0 = \tilde{a}'_0$ for the case $\epsilon = 0$. Hence our result is in agreement with Siekmann (1962), observing that

$$B_n = (-1)^n B^*_n, \quad C_n = (-1)^{n+1} C^*_n,$$

where the coefficients B^*_n and C^*_n are those used by Siekmann.

We want to calculate now the time average value of the thrust over a period of $T_0 = 2\pi/\omega$. The time average value of an arbitrary function of time $\Omega(t)$ is defined as

$$\mathring{\Omega} = \frac{1}{T_0} \int_0^{T_0} \Omega(t)\, dt. \tag{13.21}$$

Thus

$$\mathring{\Omega}_1 = \frac{1}{T_0} \int_0^{T_0} \cos^2 \omega t\, dt = \tfrac{1}{2}, \quad \mathring{\Omega}_2 = \frac{1}{T_0} \int_0^{T_0} \sin^2 \omega t\, dt = \tfrac{1}{2},$$
$$\mathring{\Omega}_3 = \frac{1}{T_0} \int_0^{T_0} \sin \omega t \cos \omega t\, dt = 0. \tag{13.22}$$

Hence, we find for example

$$\frac{1}{T_0} \int_0^{T_0} \tilde{a}'_n \tilde{B}'_m\, dt = \tfrac{1}{2}(a'_n B'_m + a''_n B''_m), \tag{13.23a}$$

$$\frac{1}{T_0} \int_0^{T_0} \tilde{C}'_n \tilde{C}'_m\, dt = \tfrac{1}{2}(C'_n C'_m + C''_n C''_m), \tag{13.23b}$$

etc., and also

$$\frac{1}{T_0} \int_0^{T_0} \sum_{n=1}^{\infty} n \tilde{B}'_n \tilde{B}''_n\, dt = 0. \tag{13.24}$$

Next we define B_* to be

$$B_* = \frac{1}{T_0} \int_0^{T_0} \sum_{n=1}^{\infty} n (\tilde{B}''_{n-1} + \tilde{B}''_{n+1}) \tilde{B}'_n\, dt$$
$$= \frac{1}{2} \sum_{n=1}^{\infty} n [(B''_{n-1} + B''_{n+1}) B'_n - (B'_{n-1} + B'_{n+1}) B''_n], \tag{13.25}$$

and C_* to be

$$C_* = \frac{1}{T_0}\int_0^{T_0} \sum_{n=1}^{\infty} \frac{1}{2n} (\tilde{C}''_{|n-2|} - \tilde{C}''_{n+2})(\tilde{C}'_{n-1} - \tilde{C}'_{n+1})\, dt$$

$$= \frac{1}{4}\sum_{n=1}^{\infty} \frac{1}{n} [C''_{|n-2|}(C'_{n-1} - C'_{n+1}) - C'_{|n-2|}(C''_{n-1} - C''_{n+1}) + C''_{n+2}(C'_{n+1} - C'_{n-1}) - C'_{n+2}(C''_{n+1} - C''_{n-1})]. \quad (13.26)$$

Substituting these results into equation (13.20) and defining a thrust coefficient by

$$C_T = \dot{\bar{F}}_x / \pi\rho U^2$$

we find the time average value of the thrust coefficient C_T to be

$$\begin{aligned} C_T = {} & (r'_0 + C'_0)(r'_0 - C'_1) + (r''_0 + C''_0)(r''_0 - C''_1) + k^2(B'_0 B'_1 + B''_0 B''_1) \\ & - \epsilon[2(r'_0 - 2A'_0 + 2A'_1)(C'_0 - C'_1) + 2(r''_0 - 2A''_0 + 2A''_1)(C''_0 - C''_1) \\ & + 3(C'_0 C'_1 + C''_0 C''_1 - C'^2_0 - C''^2_0 + C'^2_1 + C''^2_1) + r'^2_0 + r''^2_0] \\ & - \epsilon[k^2(B'_0 B'_1 + B''_0 B''_1 - B'^2_1 - B''^2_1 - B'_0 B'_2 - B''_0 B''_2) + k(B_* + C_*)], \quad (13.27) \end{aligned}$$

where

$$r'_0 = (A'_0 + A'_1)\mathfrak{F}(\Lambda k) - (A''_0 + A''_1)\mathfrak{G}(\Lambda k) - A'_1,$$

$$r''_0 = (A''_0 + A''_1)\mathfrak{F}(\Lambda k) + (A'_0 + A'_1)\mathfrak{G}(\Lambda k) - A''_1.$$

14. Numerical example

In order to compare this work with previous results for a very thin plate (Siekmann 1962) we take a displacement function with a quadratic amplitude in the form

$$D(z,t) = ih(x,t) = i(d_0 + d_1 x + d_2 x^2)\, e^{-j\alpha x} e^{j\omega t}. \quad (14.1)$$

Here the phase angle Δ_0 is set equal to zero. From equation (11.1) it follows that

$$x = (1-\epsilon)\cos\vartheta + \tfrac{1}{2}\epsilon. \quad (14.2)$$

Combining these expressions with equation (5.11) we get, after some straightforward calculations,

$$\begin{aligned} H_1^*(\vartheta) = {} & [(d_0 + \tfrac{1}{2}\epsilon d_1 + \tfrac{1}{2}(1-\epsilon)^2 d_2)(\cos\tfrac{1}{2}\alpha\epsilon - j\sin\tfrac{1}{2}\alpha\epsilon) \\ & + (1-\epsilon)(d_1 + \epsilon d_2)(\cos\tfrac{1}{2}\alpha\epsilon - j\sin\tfrac{1}{2}\alpha\epsilon)\cos\vartheta \\ & + \tfrac{1}{2}(1-\epsilon)^2 d_2 (\cos\tfrac{1}{2}\alpha\epsilon - j\sin\tfrac{1}{2}\alpha\epsilon)\cos 2\vartheta]\, e^{-j\alpha(1-\epsilon)\cos\vartheta}. \quad (14.3) \end{aligned}$$

Substituting this result into equation (5.15) and employing the integral

$$J_n(\kappa) = j^{-n}\frac{1}{\pi}\int_0^{\pi} e^{j\kappa\cos\vartheta}\cos n\vartheta\, d\vartheta, \quad (14.4)$$

where $\kappa = (1-\epsilon)\alpha$ and $J_n(\kappa)$ is the Bessel function of order n, we obtain after some straightforward manipulations the real and imaginary parts of the B_n Fourier coefficients,

$$B_n = \frac{1}{\pi}\int_0^{\pi} H_1^*(\vartheta)\cos n\vartheta\, d\vartheta,$$

as follows:

$$B_0' = [d_0 + \tfrac{1}{2}\epsilon d_1 + \tfrac{1}{2}(1-\epsilon)^2 d_2]\cos\tfrac{1}{2}\alpha\epsilon\, J_0(\kappa) + (1-\epsilon)(d_1+\epsilon d_2)\sin\tfrac{1}{2}\alpha\epsilon\, J_1(\kappa) + \tfrac{1}{2}(1-\epsilon)^2 d_2 \cos\tfrac{1}{2}\alpha\epsilon[J_0(\kappa) - 2\kappa^{-1}J_1(\kappa)], \tag{14.5a}$$

$$B_0'' = -[d_0 + \tfrac{1}{2}\epsilon d_1 + \tfrac{1}{2}(1-\epsilon)^2 d_2]\sin\tfrac{1}{2}\alpha\epsilon J_0(\kappa) - (1-\epsilon)(d_1+\epsilon d_2)\cos\tfrac{1}{2}\alpha\epsilon J_1(\kappa) - \tfrac{1}{2}(1-\epsilon)\, d_2 \sin\tfrac{1}{2}\alpha\epsilon[J_0(\kappa) - 2\kappa^{-1}J_1(\kappa)], \tag{14.5b}$$

$$B_{2n+1}' = (-1)^{n+1}\{[d_0 + \tfrac{1}{2}\epsilon d_1 + \tfrac{1}{2}(1-\epsilon)^2 d_2]\sin\tfrac{1}{2}\alpha\epsilon J_{2n+1}(\kappa) + (1-\epsilon)(d_1+\epsilon d_2)\cos\tfrac{1}{2}\alpha\epsilon[(2n+1)\kappa^{-1}J_{2n+1}(\kappa) - J_{2n}(\kappa)] + \tfrac{1}{2}(1-\epsilon)^2 d_2 \sin\tfrac{1}{2}\alpha\epsilon[(1 - 2(2n+1)\kappa^{-2} - 2(2n+1)^2\kappa^{-2})J_{2n+1}(\kappa) + 2\kappa^{-1}J_{2n}(\kappa)]\}, \tag{14.5c}$$

$$B_{2n+1}'' = (-1)^{n+1}\{[d_0 + \tfrac{1}{2}\epsilon d_1 + \tfrac{1}{2}(1-\epsilon)^2 d_2]\cos\tfrac{1}{2}\epsilon\alpha J_{2n+1}(\kappa) - (1-\epsilon)(d_1+\epsilon d_2)\sin\tfrac{1}{2}\alpha\epsilon[(2n+1)\kappa^{-1}J_{2n+1}(\kappa) - J_{2n}(\kappa)] + \tfrac{1}{2}(1-\epsilon)^2 \times d_2 \cos\tfrac{1}{2}\alpha\epsilon[(1 - 2(2n+1)\kappa^{-2} - 2(2n+1)^2\kappa^{-2})J_{2n+1}(\kappa) + 2\kappa^{-1}J_{2n}(\kappa)]\}, \tag{14.5d}$$

$$B_{2n}' = (-1)^n\{[d_0 + \tfrac{1}{2}\epsilon d_1 + \tfrac{1}{2}(1-\epsilon)^2 d_2]\cos\tfrac{1}{2}\alpha\epsilon J_{2n}(\kappa) - (1-\epsilon)(d_1+\epsilon d_2)\sin\tfrac{1}{2}\alpha\epsilon[2n\kappa^{-1}J_{2n}(\kappa) - J_{2n-1}(\kappa)] + \tfrac{1}{2}(1-\epsilon)^2 d_2 \cos\tfrac{1}{2}\alpha\epsilon \times [1 - 2(2n)\kappa^{-2} - 2(2n)^2\kappa^{-2}J_{2n}(\kappa) + 2\kappa^{-1}J_{2n-1}(\kappa)]\}, \tag{14.5e}$$

$$B_{2n}'' = (-1)^{n-1}\{[d_0 + \tfrac{1}{2}\epsilon d_1 + \tfrac{1}{2}(1-\epsilon)^2 d_2]\sin\tfrac{1}{2}\alpha\epsilon J_{2n}(\kappa) + (1-\epsilon)(d_1+\epsilon d_2)\cos\tfrac{1}{2}\alpha\epsilon[2n\kappa^{-1}J_{2n}(\kappa) - J_{2n-1}(\kappa)] + \tfrac{1}{2}(1-\epsilon)^2 d_2 \sin\tfrac{1}{2}\alpha\epsilon \times [(1 - 2(2n)\kappa^{-2} - 2(2n)^2\kappa^{-2})J_{2n}(\kappa) + 2\kappa^{-1}J_{2n-1}(\kappa)]\}. \tag{14.5f}$$

In establishing these results the following recurrence relations between the Bessel functions have been used:

$$J_n(-\kappa) = (-1)^n J_n(\kappa),$$
$$J_{n-1}(\kappa) + J_{n+1}(\kappa) = 2n\kappa^{-1}J_n(\kappa),$$
$$J_{n+1}(\kappa) - J_{n-1}(\kappa) = 2n\kappa^{-1}J_n(\kappa) - 2J_{n-1}(\kappa),$$

and

$$J_{n-2}(\kappa) + J_{n+2}(\kappa) = -2\left[\left(1 - \frac{2n}{\kappa^2} - \frac{2n^2}{\kappa^2}\right)J_n(\kappa) + \frac{2}{\kappa}J_{n-1}(\kappa)\right].$$

From

$$C_n = \frac{1}{\pi}\int_0^{\pi} \frac{1}{\sin\vartheta}\,\frac{dH_1^*(\vartheta)}{d\vartheta}\cos n\vartheta\, d\vartheta$$

we find in a similar manner the real and imaginary parts of the C_n Fourier coefficients to be

$$C_0' = [-(1-\epsilon)(d_1+\epsilon d_2)\cos\tfrac{1}{2}\alpha\epsilon + \kappa(d_0 + \tfrac{1}{2}\epsilon d_1 + \tfrac{1}{2}(1-\epsilon)^2 d_2)\sin\tfrac{1}{2}\alpha\epsilon]J_0(\kappa) + [\kappa(1-\epsilon)(d_1+\epsilon d_2)\cos\tfrac{1}{2}\alpha\epsilon + 2(1-\epsilon)^2 d_2 \sin\tfrac{1}{2}\alpha\epsilon]J_1(\kappa) + [\tfrac{1}{2}\kappa(1-\epsilon)^2 d_2 \sin\tfrac{1}{2}\alpha\epsilon][J_0(\kappa) - 2\kappa^{-1}J_1(\kappa)], \tag{14.6a}$$

$$C_0'' = \{(1-\epsilon)(d_1+\epsilon d_2)\sin\tfrac{1}{2}\alpha\epsilon + \kappa[d_0 + \tfrac{1}{2}\epsilon d_1 + \tfrac{1}{2}(1-\epsilon)^2 d_2]\cos\tfrac{1}{2}\alpha\epsilon\}J_0(\kappa) + [-\kappa(1-\epsilon)(d_1+\epsilon d_2)\sin\tfrac{1}{2}\alpha\epsilon + 2(1-\epsilon)^2 d_2 \cos\tfrac{1}{2}\alpha\epsilon]J_1(\kappa) + [\tfrac{1}{2}\kappa(1-\epsilon)^2 d_2 \cos\tfrac{1}{2}\alpha\epsilon][J_0(\kappa) - 2\kappa^{-1}J_1(\kappa)], \tag{14.6b}$$

$$C'_{2n+1} = (-1)^n\{[(1-\epsilon)(d_1+\epsilon d_2)\sin\tfrac{1}{2}\alpha\epsilon+\kappa(d_0+\tfrac{1}{2}\epsilon d_1+\tfrac{1}{2}(1-\epsilon)^2 d_2)\cos\tfrac{1}{2}\alpha\epsilon]J_{2n+1}(\kappa)$$
$$+[-\kappa(1-\epsilon)(d_1+\epsilon d_2)\sin\tfrac{1}{2}\alpha\epsilon+2(1-\epsilon)^2 d_2\cos\tfrac{1}{2}\alpha\epsilon][(2n+1)\kappa^{-1}J_{2n+1}(\kappa)$$
$$-J_{2n}(\kappa)]+[\tfrac{1}{2}\kappa(1-\epsilon)^2 d_2\cos\tfrac{1}{2}\alpha\epsilon][(1-2(2n+1)\kappa^{-2}-2(2n+1)^2\kappa^{-2})$$
$$\times J_{2n+1}(\kappa)+2\kappa^{-1}J_{2n}(\kappa)]\}, \tag{14.6c}$$

$$C''_{2n+1} = (-1)^{n-1}\{[-(1-\epsilon)(d_1+\epsilon d_2)\cos\tfrac{1}{2}\alpha\epsilon+\kappa(d_0+\tfrac{1}{2}\epsilon d_1+\tfrac{1}{2}(1-\epsilon)^2 d_2)\sin\tfrac{1}{2}\alpha\epsilon]$$
$$\times J_{2n+1}(\kappa)+[\kappa(1-\epsilon)(d_1+\epsilon d_2)\cos\tfrac{1}{2}\alpha\epsilon+2(1-\epsilon)^2 d_2\sin\tfrac{1}{2}\alpha\epsilon]$$
$$\times[(2n+1)\kappa^{-1}J_{2n+1}(\kappa)-J_{2n}(\kappa)]+[\tfrac{1}{2}\kappa(1-\epsilon)^2 d_2\sin\tfrac{1}{2}\alpha\epsilon]$$
$$\times[(1-2(2n+1)\kappa^{-2}-2(2n+1)^2\kappa^{-2})J_{2n+1}(\kappa)+2\kappa^{-1}J_{2n}(\kappa)]\}, \tag{14.6d}$$

$$C'_{2n} = (-1)^n\{[-(1-\epsilon)(d_1+\epsilon d_2)\cos\tfrac{1}{2}\alpha\epsilon+\kappa(d_0+\tfrac{1}{2}\epsilon d_1+\tfrac{1}{2}(1-\epsilon)^2 d_2)\sin\tfrac{1}{2}\alpha\epsilon]J_{2n}(\kappa)$$
$$+[\kappa(1-\epsilon)(d_1+\epsilon d_2)\cos\tfrac{1}{2}\alpha\epsilon+2(1-\epsilon)^2 d_2\sin\tfrac{1}{2}\alpha\epsilon][2n\kappa^{-1}J_{2n}(\kappa)-J_{2n-1}(\kappa)]$$
$$+[\tfrac{1}{2}\kappa(1-\epsilon)^2 d_2\sin\tfrac{1}{2}\alpha\epsilon][(1-2(2n)\kappa^{-2}-2(2n)^2\kappa^{-2})J_{2n}(\kappa)+2\kappa^{-1}J_{2n-1}(\kappa)]\}, \tag{14.6e}$$

$$C''_{2n} = (-1)^n\{[(1-\epsilon)(d_1+\epsilon d_2)\sin\tfrac{1}{2}\alpha\epsilon+\kappa(d_0+\tfrac{1}{2}\epsilon d_1+\tfrac{1}{2}(1-\epsilon)^2 d_2)\cos\tfrac{1}{2}\alpha\epsilon]J_{2n}(\kappa)$$
$$+[-\kappa(1-\epsilon)(d_1+\epsilon d_2)\sin\tfrac{1}{2}\alpha\epsilon+2(1-\epsilon)^2 d_2\cos\tfrac{1}{2}\alpha\epsilon][2n\kappa^{-1}J_{2n}(\kappa)$$
$$-J_{2n-1}(\kappa)]+[\tfrac{1}{2}\kappa(1-\epsilon)^2 d_2\cos\tfrac{1}{2}\alpha\epsilon][(1-2(2n)\kappa^{-2}-2(2n)^2\kappa^{-2})$$
$$\times J_{2n}(\kappa)+2\kappa^{-1}J_{2n-1}(\kappa)]\}. \tag{14.6f}$$

With the coefficients B_n and C_n known, we find the A_n coefficients from equation (10.7) to be

$$A'_0 = -k[(1-\epsilon)B''_0+2\epsilon B''_1]-\frac{1+\epsilon}{1-2\epsilon}C'_0+\frac{2\epsilon}{1-2\epsilon}C'_1, \tag{14.7a}$$

$$A''_0 = k[(1-\epsilon)B'_0+2\epsilon B'_1]-\frac{1+\epsilon}{1-2\epsilon}C''_0+\frac{2\epsilon}{1-2\epsilon}C''_1, \tag{14.7b}$$

$$A'_1 = -k[(1-\epsilon)B''_1+\epsilon(B''_0+B''_2)]-\frac{1+\epsilon}{1-2\epsilon}C'_1+\frac{\epsilon}{1-2\epsilon}(C'_0+C'_2), \tag{14.7c}$$

$$A''_1 = k[(1-\epsilon)B'_1+\epsilon(B'_0+B'_2)]-\frac{1+\epsilon}{1-2\epsilon}C''_1+\frac{\epsilon}{1-2\epsilon}(C''_0+C''_2). \tag{14.7d}$$

The numerical values of these coefficients were computed on the IBM 709 Electronic Computer at the University of Florida Computer Center for different sets of d_i ($i = 1, 2, 3$) coefficients and for several values of the thickness parameter. With these values known, the thrust coefficient was computed for the selected data. Figure 10 shows plots of the calculations and reported experimental data (Siekmann 1962).

The curve for $\epsilon = 0$ coincides with Siekmann (1962, figure 4). Numerical results for five values of thickness parameters are tabulated in table 2.

15. Conclusion

Based upon the theory developed and the numerical results obtained, the following observations can be made:

(1) The thickness of the two-dimensional fish tends to reduce the available thrust generated by the swimming motion. This phenomenon indicates that a

slender fish apparently has more available progressive force in which to manoeuvre than does a fat fish of comparable length. Of course, in order to obtain the net thrust available the viscous effects must be considered.

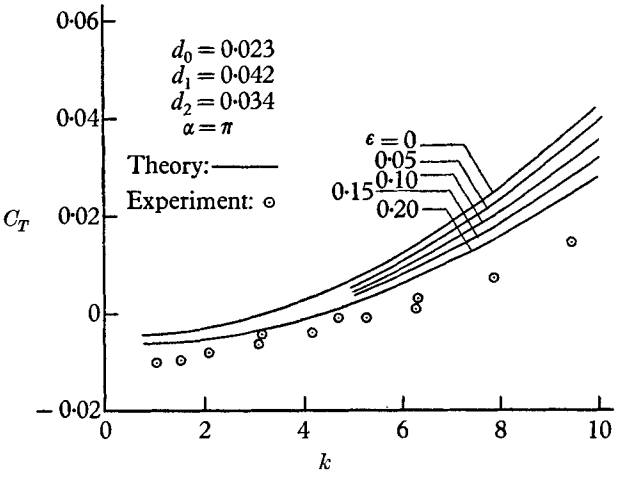

FIGURE 10. Thrust coefficient *vs* reduced frequency for quadratic amplitude.

k	$\epsilon = 0{\cdot}00$	$\epsilon = 0{\cdot}05$	$\epsilon = 0{\cdot}10$	$\epsilon = 0{\cdot}15$	$\epsilon = 0{\cdot}20$
1	−0·0044	−0·0051	−0·0055	−0·0058	−0·0059
2	−0·0030	−0·0038	−0·0043	−0·0046	−0·0048
3	−0·0007	−0·0016	−0·0022	−0·0026	−0·0030
4	0·0026	0·0016	0·0007	0·0001	−0·0006
5	0·0069	0·0056	0·0045	0·0035	0·0026
6	0·0121	0·0105	0·0091	0·0078	0·0063
7	0·0183	0·0164	0·0146	0·0127	0·0108
8	0·0254	0·0231	0·0208	0·0184	0·0159
9	0·0335	0·0307	0·0279	0·0249	0·0216
10	0·0425	0·0392	0·0358	0·0321	0·0280

TABLE 2. Thrust coefficient C_T.

(2) The thickness effect is pronounced at higher reduced frequencies than at smaller ones.

(3) The thrust coefficient depends upon all of the Fourier coefficients B_n and C_n for a finite thick fish instead of only two B_n's and C_n's as in the case of a fish of zero thickness.

(4) The argument of the Theodorsen function is increased by an amount depending upon the thickness of the fish. This results from the slowing-up effect of fluid particles in the wake.

(5) The present theory yields identical results for lift, moment and thrust with existing thin plate theories when the thickness parameter vanishes.

REFERENCES

BONTHRON, R. J. & FEJER, A. A. 1962 A hydrodynamic study of fish locomotion. *Proc. 4th U.S. Nat. Congr. Appl. Mech., Berkeley, California*, pp. 1249–55.

KELLY, H. R. 1961 Fish propulsion hydrodynamics. *Proc. 7th Midwestern Conf. on Fluid Mech., Michigan State University.* In *Developments in Mechanics*, **1**, pp. 442–50. New York: Plenum Press.

LIGHTHILL, M. J. 1960*a* Mathematics and aeronautics. *J. Roy. Aero. Soc.* **64**, 373–94.

LIGHTHILL, M. J. 1960*b* Note on the swimming of slender fish. *J. Fluid Mech.* **9**, 305–17.

LUKE, Y. & DENGLER, M. A. 1951 *J. Aero. Sci.* **18**, 478–83.

SIEKMANN, J. 1962 Theoretical studies of sea animal locomotion, Part 1. *Ing.-Arch.* **31**, 214–28.

SIEKMANN, J. 1963 Theoretical studies of sea animal locomotion, Part 2. *Ing.-Arch.* **32**, 40–50.

SIEKMANN, J. & PAO, S. K. 1964 Note on the Smith–Stone theory of fish propulsion. *Proc. Roy. Soc.* A (in Press).

SMITH, E. H. & STONE, D. E. 1961 Perfect fluid forces in fish propulsion: the solution of the problem in an elliptic cylinder co-ordinate system. *Proc. Roy. Soc.* A, **261**, 316–28.

THEODORSEN, T. 1934 General theory of aerodynamic instability and the mechanism of flutter. *NACA Rep.* no. 496.

WATSON, G. N. 1948 *A Treatise on the Theory of Bessel Functions*, 2nd ed. Cambridge University Press.

WU, T. Y. 1961 Swimming of a waving plate. *J. Fluid Mech.* **10**, 321–44.

WU, T. Y. 1962 Accelerated swimming of a waving plate. *4th Symp. on Naval Hydrodynamics.* Washington, D.C.